1 **The paradox of assessing greenhouse gases from soils for nature-**

2 **based solutions**

4 **Authors:**

5 Rodrigo Vargas[1*] and Van Huong Le[1]

7 **Affiliations**

8 [1]Department of Plant and Soil Science, University of Delaware, Newark, DE, USA

11 *Corresponding Author

12 Rodrigo Vargas (rvargas@udel.edu)

21 **Abstract**

22 Quantifying the role of soils in nature-based solutions ~~require~~requires accurate estimates of

23 soil greenhouse gas (GHG) fluxes. Technological advances allow us to ~~simultaneously~~

24 measure multiple GHGs simultaneously, and now it is possible to provide complete GHG

25 budgets from soils (i.e., CO_2, CH_4, and N_2O fluxes). We propose that there is a conflict

26 between the convenience of simultaneously measuring multiple soil GHG fluxes at fixed time

27 intervals (e.g., once~~,~~ or twice per month) and the intrinsic temporal variability and patterns of

28 different GHG fluxes. Information derived from fixed time intervals -~~as is~~commonly done

29 during manual field campaigns- had limitations to ~~reproduce~~reproducing statistical

30 properties, temporal dependence, annual budgets, and associated uncertainty~~,~~ when compared

31 with information derived from continuous measurements (i.e., automated hourly

32 measurements) for all soil GHG fluxes. We present a novel approach (i.e., temporal

33 univariate Latin Hypercube sampling) that can be applied to provide insights and optimize

34 monitoring efforts of GHG fluxes across time. We suggest that multiple GHG fluxes should

35 not be simultaneously measured at a few fixed time intervals (~~especially~~mainly when

36 measurements are limited to once ~~a~~per month), but an optimized sampling approach can be

37 used to reduce bias and uncertainty. These results have implications for assessing GHG

38 fluxes from soils and consequently reduce uncertainty on the role of soils in nature-based

39 solutions.

41 **Keywords:** Carbon dioxide, methane, nitrous oxide, representativeness, uncertainty

1. Introduction

Soils are ~~important~~essential for nature-based solutions for their role in climate mitigation potential through ~~the implementation of~~implementing different natural pathways (Griscom et al., 2017; Bossio et al., 2020). The climate mitigation potential of soils is dependent on multiple factors such as weather variability (Kim et al., 2012), ecosystem type (Oertel et al., 2016), soil structure (Ball, 2013), management practices (Shakoor et al., 2021), or disturbances (Vargas, 2012), where soils can ultimately act as net sources or sinks of greenhouse gases (GHGs). Therefore, accurate quantification of the magnitudes and patterns of soil GHGs fluxes is needed to understand the potential of soils to mitigate or contribute to global warming across ecosystems and different scenarios.

Most of our understanding of soil GHGs has come from manual measurements performed throughout labor-~~-~~intensive field campaigns and experiments (Oertel et al., 2016). While most studies around the world have focused on soil CO_2 fluxes (Jian et al., 2020), ~~there are~~ early examples ~~reporting~~have reported coupled measurements of soil CO_2, CH_4, and N_2O fluxes across tropical forests (Keller et al., 1986) and savannas (Hao et al., 1988), temperate forests (Bowden et al., 1993), and peatlands (Freeman et al., 1993). These pioneer studies provided an early view of the importance of integrated measurements of multiple soil GHG fluxes to understand the net global warming potential of soils~~,~~ but also ~~demonstrate~~demonstrated the technical limitations and challenges associated with these efforts. For example, it is known that manual measurements have the strength of providing good spatial coverage during field surveys but provide limited information about the temporal variability (Yao et al., 2009; Barba et al., 2021).

Technological advances have opened the opportunity to simultaneously measure multiple soil GHG fluxes (i.e., CO_2, CH_4, and N_2O) at unprecedented temporal resolution (e.g., hourly). These efforts have demonstrated differences in diel patterns and pulse events

68   (e.g., rewetting) due to wetting and drying cycles across tropical (Butterbach-Bahl et al.,

69   2004; Werner et al., 2007), subtropical ~~(Rowlings et al., 2012)~~(Rowlings et al., 2012), and

70   temperate ~~(Savage et al., 2014; Petrakis et al., 2017)~~(Savage et al., 2014; Petrakis et al.,

71   2017) ecosystems. These approaches provide more accurate information to calculate net

72   GHG budgets and the global warming potential of soils (Capooci et al., 2019). That said,

73   performing automated measurements of multiple GHGs is expensive, and this approach

74   usually has a lower representation of the spatial heterogeneity within ecosystems (Yao et al.,

75   2009; Barba et al., 2021).

76   Ideally, we would like to measure everything, everywhere, and all the time, but this is

77   ~~not possible~~impossible due to logistical, technological, physical, and economic constraints.

78   ~~Light weight~~Lightweight and low--powered laser-based spectrometers have reduced technical

79   barriers ~~for~~to simultaneously measuring multiple GHGs fluxes from soils~~, and it~~. It is now

80   easier and faster to perform discrete manual surveys across time. This opportunity creates a

81   paradox concerning when to measure different GHG fluxes from soils when performing

82   manual measurements. ~~In general, researchers~~Researchers generally tend to perform

83   simultaneous measurements of multiple GHGs during manual surveys, but this convenience

84   could result in biased information. We propose that there is a conflict between the

85   convenience of measuring multiple GHGs at a few fixed time intervals and the intrinsic

86   temporal variability of magnitudes and patterns of different GHG fluxes.

87   Here, we present a proof-of-concept and test how a subset of measurements derived

88   from a fixed temporal stratification (FTS) for simultaneous measurements (i.e., stratified

89   sampling schedule) or using an optimized sampling (i.e., temporal univariate Latin

90   Hypercube sampling (*tuLHs*)), compared with automated measurements of soil CO_2 (F_4CO_2),

91   CH_4 (F_4CH_4), and N_2O (F_4N_2O) fluxes from a temperate forest (Petrakis et al., 2018; Barba

92   et al., 2021, 2019). ~~Here, we~~The underlying assumption supporting any FTS approach is that

a few measurements in time can reproduce the statistical properties and temporal

dependencies of soil CO_2, CH_4, and N_2O fluxes because these GHGs respond similarly to

biological and physical drivers. The *tuLHs* is a new optimization approach to reproduce the

probability distribution and the temporal dependence of each original time series of GHG

fluxes. We reveal that reporting GHG fluxes using an FTS for simultaneous measurements

may result in biased information on temporal patterns and magnitudes. This study shows how

a biased sampling schedule could influence our understanding of GHG fluxes and, ultimately,

the climate mitigation potential of soils.

~~test how a subset of measurements derived from a fixed temporal stratification (FTS)~~

~~for simultaneous measurements (i.e., stratified sampling schedule) or using an optimized~~

~~sampling (i.e., temporal univariate Latin Hypercube sampling (*tuLHs*)), compared with~~

~~automated measurements of soil CO_2 ($F_A CO_2$), CH_4 ($F_A CH_4$), and N_2O ($F_A N_2O$) fluxes in a~~

~~temperate forest. We reveal that reporting measurements of GHG fluxes using a FTS for~~

~~simultaneous measurements, results in biased information of temporal patterns and~~

~~magnitudes. This study shows how a biased sampling schedule could influence our~~

~~understanding of GHG fluxes and ultimately the climate mitigation potential of soils.~~

2. Materials and Methods

2.1 Study site

The experiment was performed in a temperate forest located at the St Jones Estuarine

Reserve (a component of the Delaware National Estuarine Research Reserve [DNERR] in

Delaware, USA. The site has a mean annual temperature of 13.3 °C and a mean annual

precipitation of 1119 mm. Soils are classified as Othello silt loam with a texture of 40% sand,

48% silt, and 12% clay within the first 10 cm (Petrakis et al., 2018). The dominant plant

species are bitternut hickory (*Carya cordiformis*), eastern red cedar (*Juniperus virginiana* L.),

118 American holly (*Ilex opaca*), sweet gum (*Liquidambar styraciflua* L.), and black gum (*Nyssa*

119 *sylvatica* (Marshall)). The site has a mean tree density of 678 stems ha^{-1} and a diameter at

120 breast height (DBH) of 25.7±13.9 cm (mean±SD) (Barba et al., 2021).

121

122 *2.2 Automated measurements of soil GHG fluxes*

123 We ~~performed~~analyzed data from automated measurements (~~45 minutes~~1hr time intervals) of

124 soil emissions of three GHGs (i.e., CO_2, CH_4, and N_2O) between ~~September 2014 –~~

125 ~~September~~January and December 2015. This was a typical year with a mean annual

126 temperature of 13.4 °C and an annual precipitation of 1232 mm. Continuous measurements

127 of soil GHGs were taken by coupling a closed-path infrared gas analyzer (Li-COR LI-8100

128 A, Lincoln, Nebraska) and nine dynamic soil chambers (Li-COR 8100–104) controlled by a

129 multiplexer (Li-COR 8100-104) with a cavity ring-down spectrometer (Picarro G2508, Santa

130 Clara, California). ~~Detailed description of experimental design, measurements protocol are~~

131 ~~described in previous studies~~A detailed description of the experimental design and

132 measurements protocol is described in previous studies (Petrakis et al., 2018; Barba et al.,

133 2021, 2019). Briefly, for each flux observation, we measured CO_2, CH_4 ~~(Petrakis et al.,~~

134 ~~2018; Barba et al., 2021, 2019). Briefly, for each flux observation, we measured CO_2, CH_4~~

135 and N_2O concentrations every second with the Picarro G2508 for 300 seconds and calculated

136 fluxes (at ~~45 minutes~~1 hr time intervals) from the mole dry fraction of each gas (i.e.,

137 corrected for water vapor dilution) using the SoilFluxPro software (v4.0; Li-COR, Lincoln,

138 Nebraska, USA). Fluxes were estimated using ~~both~~ linear and exponential fits, and we kept

139 the flux calculation with the highest R^2. We applied quality assurance and quality control

140 protocols using information from all three GHGs as established in previous studies (Petrakis

141 et al., 2018; Barba et al., 2021, 2019; Capooci et al., 2019; Petrakis et al., 2017). Using these

142 time series, we extracted values to represent discrete temporal measurements based on FTS

143 and ~~using an~~used the optimization approach ~~as~~ described below.

144

145 *2.3 Temporal subsampling of time series*

146 Subsampling of time series was performed using FTS and a temporal optimization following

147 a univariate Latin Hypercube (*tuLHs*) approach. The difference between FTS and temporal

148 optimization is that the first approach is focused on a fixed schedule (e.g., sampling once per

149 month), and the second is focused on reproducing the statistical properties and temporal

150 dependence relationship of the original GHG time series with a subset of measurements. This

151 means ~~that~~ optimized subsamples may not be spaced systematically (e.g., every 15 days~~)~~),

152 and selected dates may vary for each GHG flux due to their specific statistical properties and

153 temporal ~~variability~~dependence.

154   FTS represents a traditional schedule for performing manual measurements of GHG

155 fluxes from soils. The FTS is usually performed with manual measurements because they

156 require extensive logistical coordination due to travel time and costs, availability of

157 instrumentation (e.g., gas analyzers~~) and~~), personnel to perform the measurements, and

158 weather conditions. During these scheduled visits, researchers usually collect fluxes from all

159 three GHGs and analyze them ~~in a systematic manner~~systematically to calculate magnitudes

160 and patterns throughout the ~~length of the~~ experiment. Usually, researchers perform manual

161 samples during the early hours of the day (between 9 am and 12 pm) to avoid confounding

162 effects due to large changes in temperature and moisture, as demonstrated by information

163 summarized by the soil respiration global database (Cueva et al., 2017; Jian et al., 2020).

164 Consequently, we selected subsamples from each original GHG time series (derived from

165 automated measurements) using flux measurements from 10 am at fixed intervals of once per

166 month (n=12), twice per month (n=24), or four times per month (n=48) starting on the first

167 week of available data from automated measurements.

168 We applied *tuLHs* as an alternative subsampling approach to obtain an optimized

169 subsample with the same univariate statistical properties and temporal dependence

170 relationship of the original GHG time series. Optimization was performed to select

171 subsamples for each GHG flux using the same number of samples as for ~~fix temporal~~

172 ~~stratification~~FTS: twelve ($k=12$), twenty-four ($k=24$~~)~~), or forty-eight ($k=48$) measurements

173 throughout the year of available data from automated measurements.

174

175 *2.4 Temporal Univariate Latin Hypercube Sampling (tuLHs)*

176 Let $S = \{(x_1, y_1, z_1), (x_2, y_2, z_2), \ldots, (x_n, y_n, z_n)\}$ be observations of the variables X, Y, and Z in a

177 time series, where X, Y, and Z are soil GHGs (i.e., CO_2, CH_4, and N_2O). Each measured

178 variable ~~of the time series~~ is characterized by ~~two functions:~~ the univariate probability

179 distribution function and the temporal dependency function. Once these two functions are

180 known, then the behaviors of the variable can be reproduced ~~(Le et al., 2020; Chilès and~~

181 ~~Delfiner, 2009; Trangmar et al., 1986; Pyrcz and Deutsch, 2014)~~(Le et al., 2020; Chilès and

182 Delfiner, 2009; Trangmar et al., 1986; Pyrcz and Deutsch, 2014). The *tuLHs* consists of three

183 steps: (1) modeling the univariate behavior of the variable using the empirical cumulative

184 univariate probability distribution function; (2) modeling the temporal dependence using the

185 empirical variogram function; and (3) optimizing a subsample applying a global optimization

186 method, differential evolution, using the previously obtained variogram function as an

187 objective function.

188 First, to model the univariate behavior of the variables from the observations of S, the

189 empirical univariate cumulative distribution function $F^*_n(x)$ of X is estimated by:

$$190 \qquad F_n^*(x) = \frac{1}{n} \sum_{i=1}^{n} I\{x_i \leq x\} \qquad (1)$$

191 where *I* represents an indicator function equal to 1 when its argument is true, and 0 otherwise.

192 Similarly, the empirical univariate distribution function of the variables *Y* and *Z* can be derived.

193 Second, to model the temporal dependence of the variables from the observations of *S*, the

194 empirical temporal correlation function (i.e., temporal variogram function) $\gamma^*(t)$ of X is

195 estimated by:

$$196 \qquad \gamma^*(t) = \frac{1}{2N(t)} \sum_{i=1}^{N(t)} [X(t_i + t) - X(t_i)]^2 \qquad (2)$$

197 where *N(t)* is the number of pairs $X(t_i + t)$ and $X(t_i)$ are separated by a time *t*. The variogram

198 functions of the variables Y and Z are analogous. Third, ~~Toto~~ to optimize the subsample, it is

199 required to choose the "optimal" data points with the selected sample size (i.e., *k*=12, 24, or

200 48; where *k* << *n)* that will have the same behavior ~~of~~as the original observations of *S* (i.e.,

201 GHG fluxes derived from automated measurements). To achieve this objective, we use ~~the~~

202 differential evolution, a global optimization method ~~(Storn and Price, 1997)~~(Storn and Price,

203 1997), using the variogram function as an objective function. The procedure consists of

204 dividing the univariate empirical probability distribution in Eq. (1) into *k* equiprobable strata,

205 which is equivalent to k ordered data subsets. From each subset, only one value must be chosen

206 to satisfy the condition of a univariate Latin hypercube. The differential evolution method is

207 applied to find the optimal points that minimize the difference between the subsample

208 variogram γ (t) and the data variogram γ * (t) in Eq. (3).

$$209 \qquad OF_1 = \sum_{i=1}^{N(t)} [\gamma(t) - \gamma^*(t)]^2 \qquad (3)$$

210 where *OF* is the objective function, and the variograms γ (t) and γ * (t) are calculated using Eq.

211 (2).

212

2.5 Statistical analyses

The t-test was used to compare the means, and the Kolmogorov-Smirnov test was used to

compare the probability distribution of measurements derived from each ~~different~~ sampling

protocol. All tests were done with ~~the~~a 95% confidence level. In addition, their statistical

properties, such as mean, median, standard deviation, and first and third quartile ~~are~~, were

compared. The differences ~~of~~in the experimental semivariograms were calculated as a

comparison measure for the temporal dependence of the samples and the original time series

of GHG fluxes. For cumulative sums of GHG flux, their mean is calculated as the most likely

value ~~and their quantile difference between 97.5 and 2.5 is used to quantify the range of~~

~~uncertainty.~~, and their quantile difference between 97.5 and 2.5 is used to quantify the range

of uncertainty. All analyzes were performed using the R program (Team and Others, 2013).

3. Results

3.1 Relationships among GHG fluxes from soils

Justification in support of FTS for simultaneous measurements of GHG fluxes would require

evidence of strong linear correlations between magnitudes and temporal dependence among

soil GHG fluxes. First, we did not find strong linear relationships between any combination

of GHG fluxes from soils derived from automated measurements (Fig. ~~A1~~S1). Therefore, our

data did not support the assumption that the magnitude of one GHG flux was associated with

a linear increase or decrease of another GHG flux. Second, semivariogram models

demonstrated differences in the temporal dependence for each GHG flux. Automated

measurements of soil CO_2 fluxes ($F_A CO_2$) showed a temporal dependence following a

Gaussian variogram model, with a nugget of 4, a sill plus nugget of 28, and a correlation

range of 80 days (Fig. ~~A2a~~S2a). Automated measurements of soil CH_4 fluxes ($F_A CH_4$) also

237 showed a temporal dependence but followed a spherical variogram model, with a nugget of

238 7×10^{-8}, a sill plus nugget of 1.5×10^{-7}, and a correlation range of 110 days (Fig. ~~A2b~~S2b). In

239 contrast, automated measurements of soil N_2O fluxes ($F_A N_2O$) did not show a temporal

240 dependence, where a pure nugget effect was present, and with a correlation range of 0 days

241 (Fig. ~~A2c~~S2c). Consequently, ~~the~~these GHG fluxes' magnitudes and temporal patterns ~~of~~

242 ~~these GHG fluxes~~ were different and did not ~~provide~~ support ~~in favor of~~ FTS for

243 simultaneous measurements of GHG from soils.

244

245 *3.2 Optimization of GHG sampling protocols*

246 We applied a *tuLHs* approach to identify subsamples ~~that had~~with the same statistical

247 properties and temporal dependence for each ~~one~~ of the original GHG time series from

248 automated measurements. Subsamples were identified for twelve ($k=12$), twenty-four

249 ($k=24$~~)~~), or forty-eight ($k=48$) measurements throughout the year for each GHG time series.

250 ~~All subsamples represent measurements collected at 10 am.~~ Our results show that the

251 optimized measurement dates were different for each GHG flux (Fig. 1), and we provide

252 explicit examples for $k=24$ (Fig. 1) and $k=12$, 48 (Fig. ~~A3, A4~~S3, S4).

253 The optimized CO_2 subsamples were well distributed throughout the year for all

254 sampling scenarios (i.e., k from 12 to 48~~),~~) because $F_A CO_2$ had a strong temporal dependence

255 and a small nugget effect with respect to the sill (Fig. ~~A2a~~S2a). The optimized CH_4

256 subsamples were also relatively well distributed throughout the year, especially for scenarios

257 of $k=24$ and $k=48$, as $F_A CH_4$ also had a temporal dependence but with a higher nugget effect

258 with respect to the sill (Fig. ~~A2b~~S2b). Finally, the optimized N_2O subsamples were more

259 ~~difficult~~challenging to define, especially with a small sample size (i.e., $k=12$; Fig. ~~A3c~~S3c)

260 because $F_A N_2O$ did not have a temporal dependence (Fig. ~~A2c~~S2c).

261

262 *3.3 Differences in statistical properties and temporal dependency of subsamples*

263 Overall, there were no statistically significant differences ~~among~~between the mean values

264 derived from automated measurements and those from FTS or the *tuLHs* approach (Fig. 2 for

265 $k=24$; Fig. ~~A5~~S5 for $k=12$; Fig. ~~A6~~S6 for $k=48$; Tables ~~A1~~S1 and ~~A2~~S2). Although this appears

266 ~~to be a~~promising ~~result, the~~, more than a simple comparison of the means is ~~not enough~~needed

267 to ~~fully~~ evaluate the information derived from different sampling ~~scenarios.~~approaches. In

268 other words, it is possible to have a similar mean value without reproducing the probability

269 distribution nor the temporal dependence of the original time series (i.e., correct answer but for

270 the wrong reasons). Here, we present results based on comparing the means, standard

271 deviation, probability distributions, and semivariograms derived from automated

272 measurements and the different sampling scenarios for all GHG fluxes.

273 The mean of $F_A CO_2$ was 5.9~~,~~ µmol CO_2 m^{-2} s^{-1}, while the mean for FTS 5.5 µmol CO_2

274 m^{-2} s^{-1}~~,~~ and 5.9 µmol CO_2 m^{-2} s^{-1} for the *tuLHs* approach with $k=24$ (Fig. 3a-c). These results

275 were comparable with the means derived from FTS (5.4 and 5.4 µmol CO_2 m^{-2} s^{-1}~~),~~) and ~~from~~

276 the *tuLHs* approach (6.2 and 5.9 µmol CO_2 m^{-2} s^{-1}) using $k=12$ and $k=48$, respectively (Figs.

277 ~~A5, A6~~S5, S6; Table ~~A1~~S1). The standard deviation of $F_A CO_2$ was 3.9 and 3.2 µmol CO_2 m^{-2}

278 s^{-1} for FTS, and 3.9 µmol CO_2 m^{-2} s^{-1} for the *tuLHs* approach with $k=24$ (Figs. 3a-c). These

279 results were comparable with the standard deviations derived from FTS (3.1 and 3.3 µmol CO_2

280 m^{-2} s^{-1}~~),~~) and ~~from~~ the *tuLHs* approach (4.1 and 3.9 µmol CO_2 m^{-2} s^{-1}) using $k=12$ and $k=48$,

281 respectively (Fig. ~~A5, A6~~S5, S6; Table ~~A1~~S1). Our results show that the semivariograms of

282 optimized samples using the *tuLHs* approach closely approximate the semivariograms of

283 automated measurements for $k=24$ (Fig. 4a) and $k=12$ and 48 (Figs. ~~A7a, A8a~~S7a, S8a). These

284 results are consistent with the sums of absolute differences between the semivariograms of the

285 samples and the semivariogram of $F_A CO_2$ with differences of 69.31, 54.39, 49.42 for FTS, and

286 5.69, 1.99, 1.39 for the *tuLHs* approach for $k=12, 24, 48$, respectively (Table ~~A2~~S2).

287   The mean of F_ACH$_4$ was -0.93 nmol CH$_4$ m^{-2} s^{-1}, while -0.86 nmol CH$_4$ m^{-2} s^{-1} for FTS

288   and -0.94 nmol CH$_4$ m^{-2} s^{-1} for the *tuLHs* approach with k=24 (Fig. 3d-f). These results were

289   also comparable with the means derived from FTS (-0.83 and -0.88 nmol CH$_4$ m^{-2} s^{-1}~~,~~) and

290   ~~from~~ the *tuLHs* approach (-0.87 and -0.92 nmol CH$_4$ m^{-2} s^{-1}) using k=12 and 48, respectively

291   (Figs. ~~A5, A6~~S5, S6; Table ~~A1~~S1). The standard deviation of F_ACH$_4$ was 0.36 and 0.26 nmol

292   CH$_4$ m^{-2} s^{-1} for FTS~~,~~ and 0.34 nmol CH$_4$ m^{-2} s^{-1} for the *tuLHs* approach with k=24. These results

293   were comparable with the standard deviations derived from FTS (0.27 and 0.29 nmol CH$_4$ m^{-2}

294   s^{-1}~~,~~) and ~~from~~ the *tuLHs* approach (0.33 and 0.35 nmol CH$_4$ m^{-2} s^{-1}) using k=12 and k=48,

295   respectively (Figs. ~~A5, A6~~S5, S6; Table ~~A1~~S1). The semivariograms of optimized samples

296   using the *tuLHs* approach closely approximate the semivariogram of automated measurements

297   for k=24 (Fig. 4b) and k=12 and 48 (Figs. ~~A7b, A8b~~S7b, S8b). Consequently, the sums of

298   absolute differences between the semivariograms of the samples and the semivariogram of

299   F_ACH$_4$ were 0.63, 0.48~~,~~0.49 for FTS, and 0.06, 0.04, 0.02 for the *tuLHs* approach with k=12,

300   24, 48, respectively (Table ~~A2~~S2).

301   Finally, the mean of F_AN$_2$O was 0.45 and 0.61 nmol N$_2$O m^{-2} s^{-1} for FTS, and 0.51 nmol

302   N$_2$O m^{-2} s^{-1} for the *tuLHs* approach with k=24 (Fig. 3g-i). These results were also comparable

303   with the means derived from FTS (0.59 and 0.25 nmol N$_2$O m^{-2} s^{-1}~~,~~) and ~~from~~ the *tuLHs*

304   approach (0.58 and 0.49 nmol N$_2$O m^{-2} s^{-1}) using k=12 and 48, respectively (Figs. ~~A5, A6~~S5,

305   S6; Table ~~A1~~S1). The standard deviation of F_AN$_2$O was 1.62 and 1.97 nmol N$_2$O m^{-2} s^{-1} for

306   FTS, and 1.54 nmol N$_2$O m^{-2} s^{-1} for the *tuLHs* approach with k=24. These results were

307   comparable with the standard deviations derived from FTS (1.38 and 0.91 nmol N$_2$O m^{-2} s^{-1}~~,~~)

308   and ~~from~~ the *tuLHs* approach (1.58 and 1.54 nmol N$_2$O m^{-2} s^{-1}) using k=12 and k=48,

309   respectively (Figs. ~~A5, A6~~S5, S6; Table ~~A1~~S1). Our results show ~~that there is~~ no temporal

310   dependence for N$_2$O fluxes, but the semivariograms of optimized samples using the *tuLHs*

311   approach closely approximate the semivariogram of automated measurements for k=24 (Fig.

312   4c) and k=12 and 48 (Figs. ~~A7c, A8c~~S7c, S8c). Consistently, the sum of absolute differences

313   between the semivariograms of the samples and the semivariogram of $F_A N_2O$ were 10.01,

314   12.25, 16.75 for FTS, and 0.82, 1.13, 3.57 for the *tuLHs* approach with k=12, 24, 48,

315   respectively (Table ~~A2~~S2).

316   These results show that the *tuLHs* approach reproduced ~~with greater precision~~ the

317   probability distribution and the temporal dependence of the time series derived from automated

318   measurements with more precision than FTS for all GHGs. In the next section, we explore the

319   implications of these differences for ~~calculation of~~calculating cumulative GHG fluxes.

320

321   *3.4 Calculation of cumulative GHG fluxes*

322   We calculated the cumulative flux for all GHGs using available information from automated

323   measurements (Fig. 2; Table ~~A3~~S3). The cumulative sum for available measurements of

324    $F_A CO_2$ was 5758.5 g CO_2 m^{-2} [893.9, 13860.8; 95% CI]; for $F_A CH_4$ was -0.47 g CH_4 m^{-2} [-

325   0.81, -0.19; 95% CI]; and 0.63 g N_2O m^{-2} [-0.75, 5.19; 95% CI] for $F_A N_2O$.

326   We used the mean for each GHG flux derived from the *tuLHs* approach or the FTS to

327   calculate the cumulative sum (Table ~~A3~~S3). We found that the FTS underestimated the

328   cumulative flux (-8.4, -6.2, -7.1%) and the uncertainty (-32.6, -21.6, -19.3%) of $F_A CO_2$ for

329   k=12, 24, 48, respectively (Fig. 5a). In contrast, the *tuLHs* approach slightly overestimated

330   the cumulative flux (6.5, 1.1, 0.1%) and slightly underestimated the uncertainty (-9.1, -4.4, -

331   3.7%) for k=12, 24, 48, respectively (Fig. 5a).

332   The FTS underestimated the cumulative flux (-9.1, -6.1, -3.1%) and the uncertainty (-

333   31.8, -27.3, -15.9%) of $F_A CH_4$ for k=12, 24, 48, respectively (Fig. 5b). In contrast, the *tuLHs*

334   approach underestimated the cumulative flux (-6.1%) only for k=12, but slightly

335   underestimated the uncertainty (-15.9, -6.8, -4.5%) for k=12, 24, 48, respectively (Fig. 5b).

336   The FTS substantially underestimated the cumulative flux (-168, -170, -173%) of

337   F_AN$_2$O for k=12, 24, 48, respectively. Uncertainty was overestimated for k=12 and 24 (3.6

338   and 26%) and underestimated for k=48 (-31%; Fig. 5c). In contrast, the *tuLHs* approach

339   overestimated less the cumulative flux (29.5, 13.4, 9.1%) for k=12, 24, 48, respectively (Fig.

340   5c). This approach underestimated the uncertainty for k=12 (-11.2%) and k=24 ~~by -11.2 and~~

341   (-13.8~~%,~~%) but overestimated the uncertainty by 2.9% for k=48 (Fig. 5c). These results show

342   that the *tuLHs* approach consistently provided closer estimates for cumulative sums and

343   uncertainty ranges than ~~a~~an FTS for all GHG fluxes.

344

345   **4. Discussion**

346   Applied challenges, such as quantifying the role of soils in nature-based solutions, require

347   accurate estimates of GHG fluxes. To do this, two fundamental ~~questions~~problems exist for

348   designing environmental monitoring protocols: where ~~to measure~~ and when to measure?

349   Ultimately a monitoring protocol aims to quantify the attributes of an ecosystem~~,~~ so that it

350   can be compared in time within that ecosystem or with other ecosystems. Because we cannot

351   measure everything, everywhere, and all the time, we can argue that any monitoring protocol

352   has assumptions ~~that are~~ based on physical, economic, social, and practical reasons to address

353   a specific scientific question. These assumptions for designing monitoring protocols could

354   result in misleading, biased, or wrong conclusions, and therefore is critical to assess the

355   consequences of different monitoring efforts. As Hutchinson described in "The Concept of

356   Pattern in Ecology~~",~~," we do not always know if a given pattern is extraordinary or a simple

357   expression of something which we may learn to expect all the time ~~(Hutchinson,~~

358   ~~1953)~~(Hutchinson, 1953).

359   ~~Automated measurements of soil GHG fluxes have revolutionized our understanding~~

360   ~~of the temporal patterns and magnitudes of these fluxes in soils (Vargas et al., 2011; Savage~~

361 ~~et al., 2014; Bond-Lamberty et al., 2020; Tang et al., 2006). That said, these types of~~

362 ~~measurements have limitations to represent spatial variability and have higher equipment~~

363 ~~costs that limits their broad applicability across study sites~~ Automated measurements have

364 revolutionized our understanding of the temporal patterns and magnitudes of soil GHG fluxes

365 (Savage et al., 2014; Bond-Lamberty et al., 2020; Tang et al., 2006; Capooci and Vargas,

366 2022b). These measurements have limitations in representing spatial variability and have

367 higher equipment costs that limit their broad applicability across study sites (Vargas et al.,

368 2011)~~. Consequently, discrete manual measurements are a common approach to~~

369 ~~simultaneously measure multiple GHG fluxes and report patterns, budgets, and information~~

370 ~~to parameterize empirical and process based models (Phillips et al., 2017; Wang and Chen,~~

371 ~~2012). In this study, we argue that the convenience of simultaneously measuring multiple~~

372 ~~GHGs using FTS may result in bias estimates; therefore, optimization of sampling protocols~~

373 ~~is needed when there is a limited number of measurements in time (i.e., $k=12, 24, 48$).~~

374 ~~We show that the magnitude of one GHG flux is not associated with a linear increase~~

375 ~~or decrease of another GHG flux, and the temporal dependencies of each GHG flux are~~

376 ~~different from each other (Fig. A1). Therefore, it is not possible to infer the dynamics of one~~

377 ~~GHG flux based solely on information from another under the assumption that they share~~

378 ~~similar (or autocorrelated) biophysical drivers. Multiple studies have shown that the~~

379 ~~importance of different biophysical drivers (e.g., temperature, moisture, light) is different for~~

380 ~~soil CO_2, CH_4 or N_2O fluxes (Luo et al., 2013; Tang et al., 2006; Ojanen et al., 2010). Our~~

381 ~~results show that soil CO_2 fluxes have a strong temporal dependence (Fig. A2a), likely as a~~

382 ~~result of the strong relationship between these fluxes and soil temperature in temperate mesic~~

383 ~~ecosystems (Hill et al., 2021; Bahn et al., 2010). The temporal dependence decreased for soil~~

384 ~~CH_4 fluxes (Fig. A2b),where there is less evidence for such strong correlation with soil~~

385 ~~temperature (Bowden et al., 1998; Castro et al., 1995), and where multiple variables are~~

386 ~~usually needed to explain the variability of these fluxes (Luo et al., 2013; Castro et al., 1994).~~

387 ~~Soil N₂O fluxes had no temporal dependence (Fig. A2c), showing a strong decoupling from~~

388 ~~soil CO₂ and CH₄ fluxes (Wu et al., 2010), likely as a result of independent biophysical~~

389 ~~drivers regulating soil N₂O fluxes (Luo et al., 2013; Bowden et al., 1993; Ullah and Moore,~~

390 ~~2011).~~

391   ~~To address the limitations of a~~. Consequently, discrete manual measurements

392 are a common approach to simultaneously measure multiple GHG fluxes and report patterns,

393 budgets, and information to parameterize empirical and process-based models (Phillips et al.,

394 2017; Wang and Chen, 2012). In this study, we argue that the convenience of simultaneously

395 measuring multiple GHGs using FTS may result in biased estimates. Therefore, optimization

396 of sampling protocols is needed to provide insights to improve measurement protocols when

397 there is a limited number of measurements in time (i.e., k=12, 24, 48).

398   We show that the magnitude of one GHG flux is not associated with a linear increase

399 or decrease of another GHG flux, and the temporal dependencies of each GHG flux are

400 different (Fig. S1). Therefore, it is not possible to infer the dynamics of one GHG flux based

401 solely on information from another under the assumption that they share similar (or

402 autocorrelated) biophysical drivers. These results imply that the magnitudes and temporal

403 patterns of GHGs are different and therefore do not support an FTS approach for

404 simultaneous measurements of GHG fluxes from soils.

405   Multiple studies have shown that the relevance of different biophysical drivers (e.g.,

406 temperature, moisture, light) is different for soil CO_2, CH_4, or N_2O fluxes (Luo et al., 2013;

407 Tang et al., 2006; Ojanen et al., 2010). Our results show that soil CO_2 fluxes have a strong

408 temporal dependence (Fig. S2a), likely due to the strong relationship between these fluxes

409 and soil temperature in this and other temperate mesic ecosystems (Hill et al., 2021; Bahn et

410 al., 2010; Barba et al., 2019). The temporal dependence decreased for soil CH_4 fluxes (Fig.

S2b), where there is less evidence for such a strong correlation with soil temperature in this and other temperate mesic ecosystems (Bowden et al., 1998; Castro et al., 1995; Warner et al., 2019; Barba et al., 2019). It has been reported that multiple variables and complex relationships are usually needed to explain the variability of soil CH_4 fluxes in forest soils, as there is a delicate balance between methanogenesis and methanotrophy (Luo et al., 2013; Castro et al., 1994; Murguia-Flores et al., 2018). In contrast, soil N_2O fluxes had no temporal dependence (Fig. S2c), showing decoupling from the observed patterns of soil CO_2 and CH_4 fluxes (Wu et al., 2010), likely as a result of independent biophysical drivers regulating soil N_2O fluxes (Luo et al., 2013; Bowden et al., 1993; Ullah and Moore, 2011).

To address the limitations of an FTS protocol, we propose a novel optimization approach (i.e., *tuLHs*) to reproduce the probability distribution and the temporal dependence of each original time series of GHG fluxes. Traditional ~~approaches~~methods usually optimize subsamples by either individually focusing on reproducing the probability distribution of the original information ~~(Huntington and Lyrintzis, 1998), or by focusing on~~(Huntington and Lyrintzis, 1998) or reproducing the temporal dependence of the original information ~~(Gunawardana et al., 2011).~~(Gunawardana et al., 2011). The *tuLHs* is a simple approach that ~~consists of using~~uses the univariate probability distribution function and the temporal correlation function (i.e., variogram) as objective functions for each GHG flux. Our results show that optimized subsamples do not coincide in time for the three GHGs, suggesting that information should be collected based on ~~the~~each GHG flux's specific statistical and temporal characteristics ~~of each GHG flux~~ (Fig. 1). This study provides ~~a~~proof-of-concept for the application of the *tuLHs* ~~and~~. It demonstrates how an optimization ~~can be performed~~approach provides insights to design monitoring protocols and improve soil GHG flux estimates ~~of soil GHG fluxes~~.

435   The more temporal data we can collect, the better, but in many cases, measurement

436   protocols are limited to a few measurements per year (i.e., k=12 to 48). Our results

437   demonstrate that for a small sample size (i.e., k=12)), the optimized measurements for soil

438   CO_2 fluxes are consistently spread across the year, and for soil CH_4 fluxes are centered

439   within the growing season, and for soil because of their strong temporal dependence. For the

440   case of soil N_2O fluxes, the variogram shows a constant temporal variability, meaning there

441   is no temporal dependence. Therefore, the optimized measurements are concentrated within

442   the fall season due to their distribution probability (Fig. 1a). Our optimization approach

443   shows how measurements can be distributed across time as more samples are available (i.e.,

444   k=24 to 48; Fig. 1b-c) and demonstrates that optimization is critical when a limited number

445   of measurements are available. In other words, a few measurements properly distributed

446   across time provide better agreement with information derived from automated

447   measurements. We highlight that this optimization approach should be tested across different

448   ecosystems as it will result in site-specific recommendations. That said, aA similar

449   conclusion was proposed for the spatial distribution of environmental observatory networks,

450   where a network of few sites properly distributed (e.g., across a country) improves our

451   understanding of the target variable more than a spatially biased network (Villarreal et al.,

452   2019). Thus, the need for representativeness assessment of information collected across time

453   and space is needed for accurate evaluation ofto evaluate environmental measurements and

454   quantification ofquantify nature-based solutions accurately.

455   An initial approach suggested no statistical differences among the mean flux values

456   derived from different sampling protocols. Arguably, this simplistic approach is a false

457   negative due to biased information from the FTS that does not accurately represent the

458   probability distribution and the temporal variability of soil GHG fluxes (e.g., Figs. 3-4). In

459 ~~contrast, the optimization approach resulted in closer probability distributions and temporal~~

460 ~~variabilities for all GHGs, providing additional evidence against the FTS approach.~~

461 We highlight that this optimization approach should be implemented across different

462 ecosystems as it will result in site-specific recommendations. The *tuLHs* can be applied to

463 any time series length and with any time step (e.g., hours, days), but specific results will be

464 representative of the probability distribution and the temporal dependence of the selected

465 time series. In this case study, the year chosen had typical climatological conditions and

466 demonstrates that the statistical properties of the GHG fluxes are different and do not support

467 an FTS approach. Therefore, longer time series (e.g., multi-year) may provide more robust

468 optimizations that can be applied to monitoring efforts in future years. Alternatively, forecast

469 scenarios can be predicted, and *tuLHs* can be used to suggest an optimized sampling design

470 under those assumptions. Testing the implications of potentially biased GHG flux estimates

471 should be a priority. Ideally, automated measurements should be co-located with manual

472 efforts to adequately capture the temporal and spatial variability of soil GHG fluxes at a

473 specific site.

474 There are several implications of biased monitoring protocols for ~~the~~ understanding ~~of~~

475 soil GHG fluxes and nature-based solutions. First, temporal patterns and temporal

476 dependency may ~~not be properly represented with the~~ need to be revisited for studies using

477 ~~an~~ FTS approach. Soil GHG fluxes have complex temporal dynamics that vary from diurnal

478 to seasonal and annual scales that ~~FTS is not able to~~a few measurements following an FTS

479 approach cannot reproduce ~~(Barba et al., 2019; Bréchet et al., 2021).~~(Barba et al., 2019;

480 Bréchet et al., 2021). Second, soil GHG fluxes could present hot-moments, which are

481 transient events with disproportionately high values that are often missed with ~~a~~an FTS

482 approach (Vargas et al., 2018; Butterbach-Bahl et al., 2004). Third, cumulative sums and

483 uncertainty ranges are biased or misleading when derived using ~~a~~an FTS approach ~~(Capooci~~

484 ~~and Vargas, 2022; Tallec et al., 2019; Lucas-Moffat et al., 2018). For this third point,~~

485 ~~our~~(Tallec et al., 2019; Lucas-Moffat et al., 2018; Capooci and Vargas, 2022b). Our study

486 demonstrates that an optimized approach consistently provided closer estimates for

487 cumulative sums and uncertainty ranges when compared with automated measurements (Fig.

488 5). We postulate that representing the variability of soil N_2O fluxes is more sensitive to the

489 FTS approach (>170% and >30% for cumulative sums and uncertainty ranges, respectively)

490 than for soil CH_4 and CO_2 fluxes. Fourth, it is possible that if the information derived from

491 ~~the~~an FTS approach is biased, then functional relationships could also be different from those

492 derived from automated measurements ~~(Capooci and Vargas, 2022). It has been discussed~~

493 ~~that hypothesis testing and our capability for~~(Capooci and Vargas, 2022a). It has been argued

494 that hypothesis testing and our capability of forecasting responses of soil GHG fluxes to

495 changing climate conditions is also biased with information from the FTS approach ~~(Vicca et~~

496 ~~al., 2014). Finally, because soils have a central role for~~(Vicca et al., 2014). Finally, because

497 soils have a central role in nature-based solutions within countries and across the world

498 (Griscom et al., 2017; Bossio et al., 2020), accurate measurements are required to ~~properly~~

499 ~~assess management practices, environmental variability and the contribution of GHGs from~~

500 ~~soils (Anderegg, 2021).~~assess management practices, environmental variability, and the

501 contribution of GHGs from soils.

502

503 **Conclusion**

504 ~~We highlight that we do not always know if a given pattern is extraordinary or a simple~~

505 ~~expression of something which we may learn to expect all the time (Hutchinson, 1953).~~

506 ~~Furthermore, the "Knowledge Paradox" has been recognized for soil science, where~~

507 ~~innovative knowledge has often not been accepted by or implemented in society (Bouma,~~

508 ~~2010). Here, we postulate that with emergent technologies there is a convenience of~~

509 ~~measuring multiple GHGs from soils; however, few measurements collected at fixed time~~

510 ~~intervals results in biased estimates.~~

511 We highlight that we only sometimes know if a given pattern is extraordinary or a simple

512 expression of something which we may learn to expect all the time (Hutchinson, 1953).

513 Furthermore, the "Knowledge Paradox" has been recognized in soil science, where

514 innovative knowledge has often not been accepted by or implemented in society (Bouma,

515 2010). Here, we postulate that with emergent technologies, there is a convenience of

516 measuring multiple GHGs from soils; however, few measurements collected at fixed time

517 intervals result in biased estimates.

518   We recognize that potential measurement bias ~~in measurements is dependent~~depends

519 on ~~the~~each GHG flux's magnitudes and temporal patterns ~~of each GHG flux~~ and could be

520 site-specific. Nevertheless, evaluations are needed to quantify potential bias in estimates of

521 GHG budgets and information used for model parameterization and environmental

522 assessments. Furthermore, the underlying assumption that each GHG flux responds similarly

523 to biophysical drivers may need to be tested across multiple ecosystems to quantify how few

524 measurements influence our understanding of magnitudes and temporal patterns of soil GHG

525 fluxes.

526   In this study, we present a proof-of-concept and propose a novel optimization

527 approach (i.e., temporal univariate Latin Hypercube sampling) that can be applied with site-

528 specific information of different ecosystems to improve monitoring efforts and reduce the

529 bias of GHG flux measurements across time. We highlight that constant biased

530 environmental monitoring may provide confirmatory information, which we have learned to

531 expect, but modifications of monitoring protocols could shed light ~~into extraordinary~~

532 ~~patterns. These~~ on new or unexpected patterns. These new patterns are the ones that will test

533 paradigms and push science frontiers.

534

535

Data Availability. All data used for this analysis is available at:

~~https://doi.org/10.6084/m9.figshare.19536004.v1~~https://doi.org/10.6084/m9.figshare.19536004.v1. The R code used in this study is available at: https://github.com/vargaslab/temporal-univariate-Latin-Hypercube.git

540

541

Author Contributions. R.V. conceived this study, and V.H.L. designed and performed the primary analysis with input from R.V in all phases. R.V. wrote the manuscript with ~~input~~contributions from V.H.L.

545

Competing Interest Statement. None

547

Acknowledgments. The authors thank the Delaware National Estuarine Research Reserve (DNERR~~), the personnel from~~) and the St Jones Reserve personnel for their support throughout this study. ~~Authors~~The authors acknowledge the land on which they realized this study as the traditional home of the Lenni-Lenape tribal nation (Delaware nation). This study was funded by a grant from the National Science Foundation (#1652594~~).~~

553
554
555
556) and NASA Carbon Monitoring System (80NSSC21K0964).
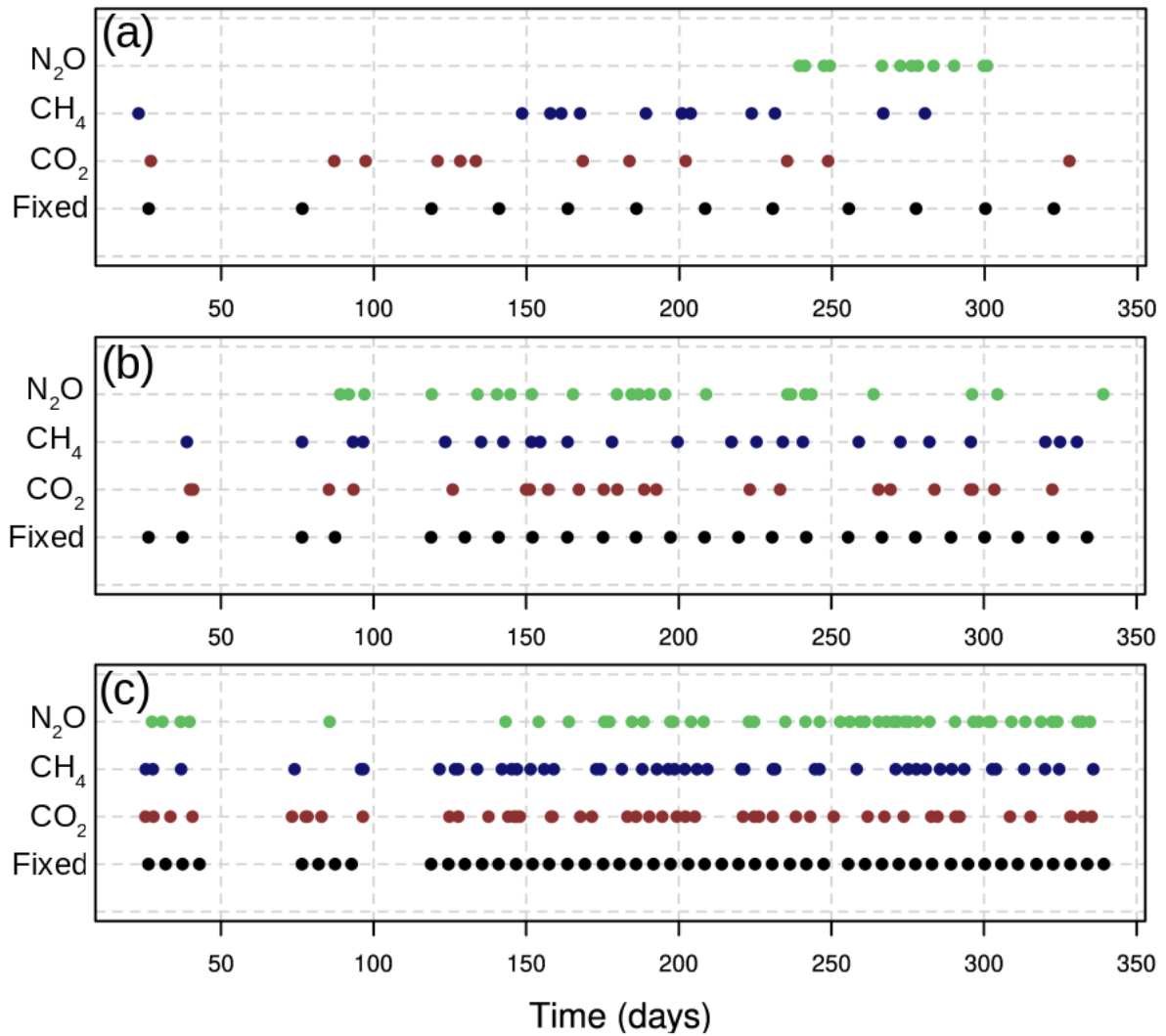
564 **Figure 1.** Temporal distribution of fixed temporal stratification (i.e., stratified manual
565 sampling approach) and optimized sampling using a temporal univariate Latin Hypercube
566 (*tuLHs*) approach for: *k*=12 (a), *k*=24 (b), and *k*=48 (c). Fixed temporal stratification is in
567 black, soil CO_2 fluxes in red, soil CH_4 fluxes in blue, and soil N_2O fluxes in green.

568   Time (x-axis) represents days from January 1 to December 31 of, 2015.
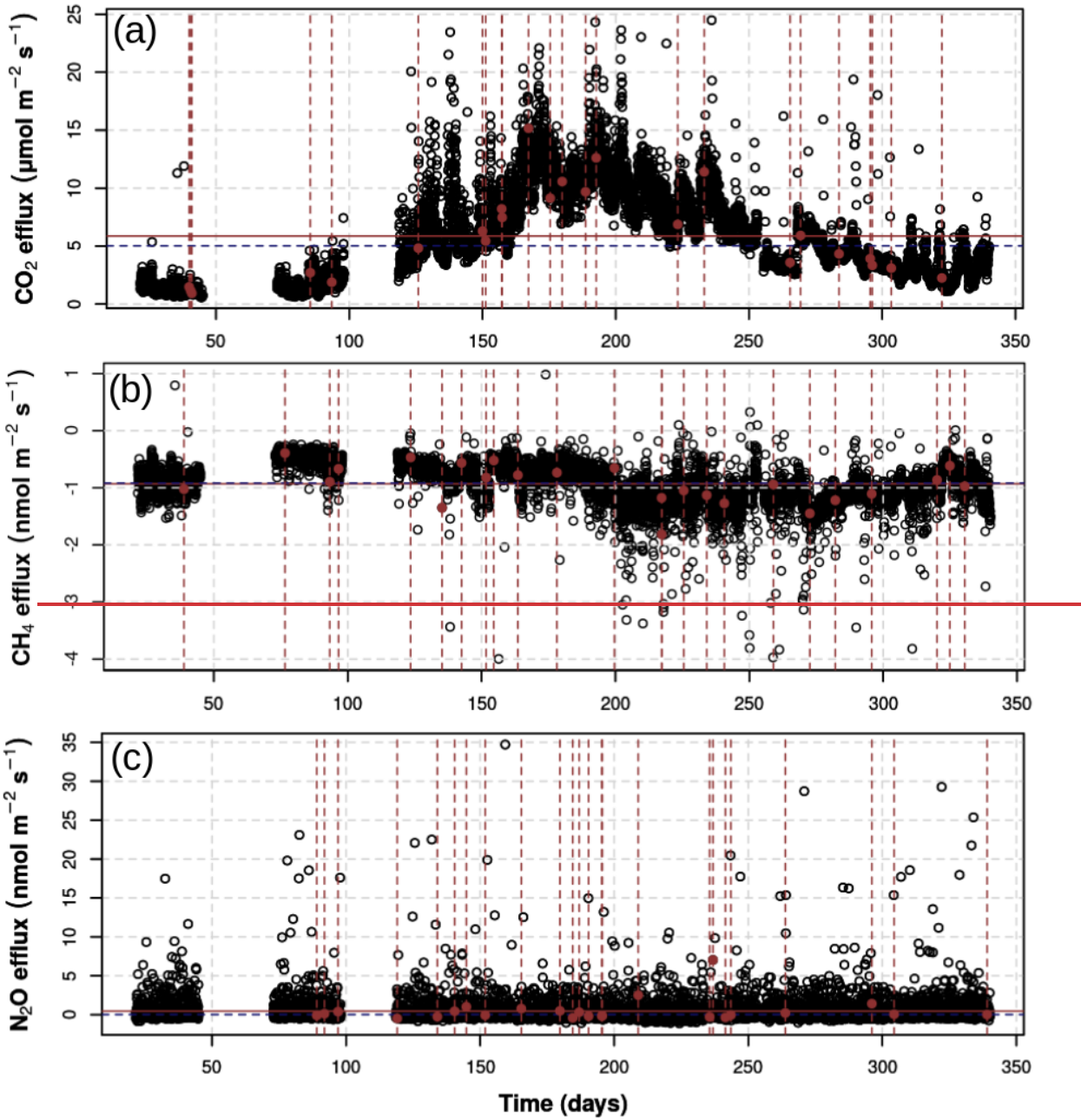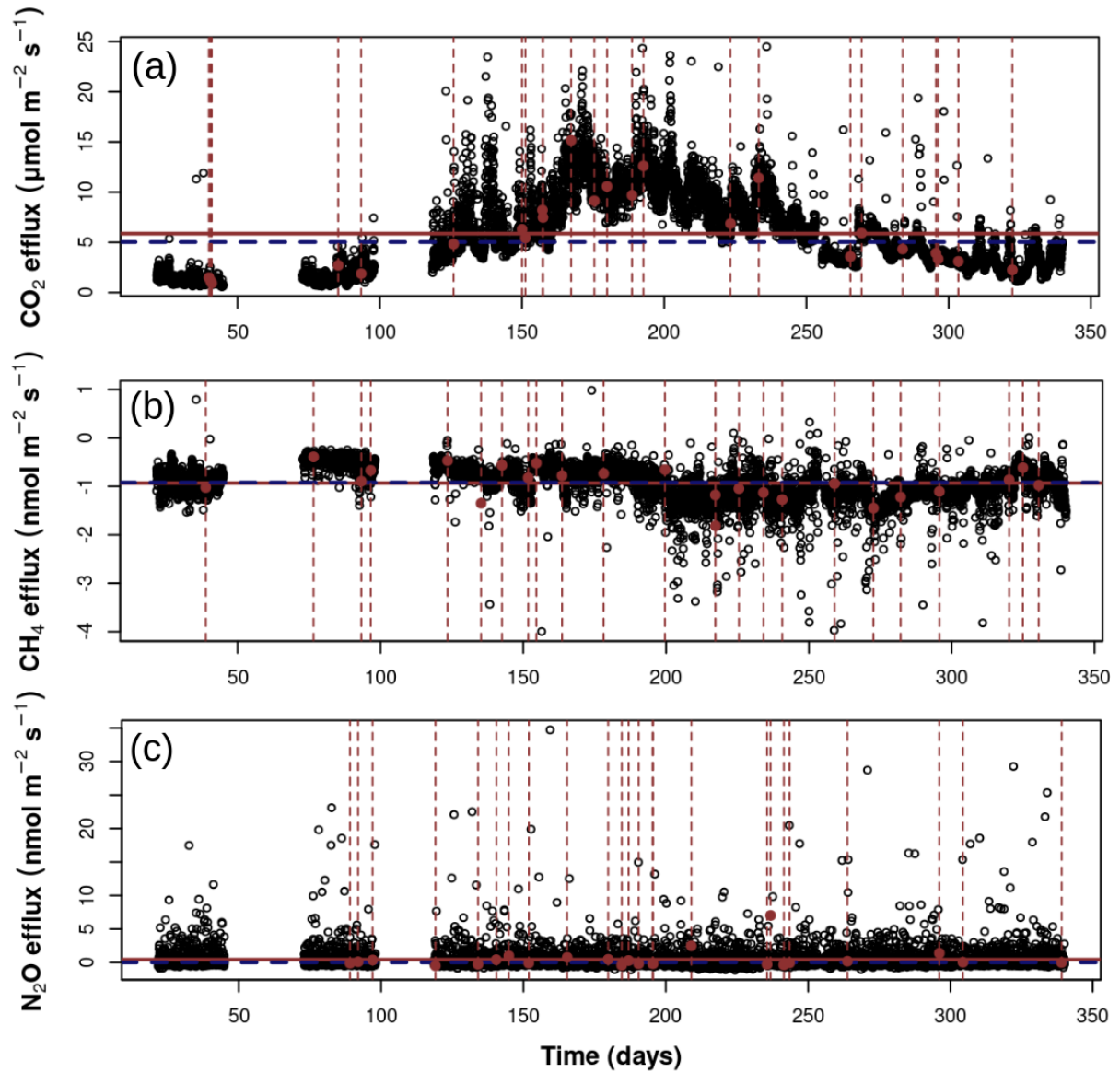
571
572
Figure 2. Time series of automated measurements (F_A) of soil greenhouse gas fluxes (black
circles) and optimized samples (k=24) using a temporal univariate Latin Hypercube sampling
(*tuLHs*) approach for soil CO_2 (a), soil CH_4 (b) and soil N_2O (c) fluxes. ~~Horizontal~~ The
horizontal red line represents the mean, and the horizontal blue line is the median of each
greenhouse gas flux derived from automated measurements. ~~Selection~~The selection of
~~datapoints~~data points for k=12 and 48 are presented for each soil greenhouse gas time series
in Figs. ~~A3~~S3 and ~~A4~~S4, respectively. Time (x-axis) represents days from January 1 to
December 31 of, 2015.

583
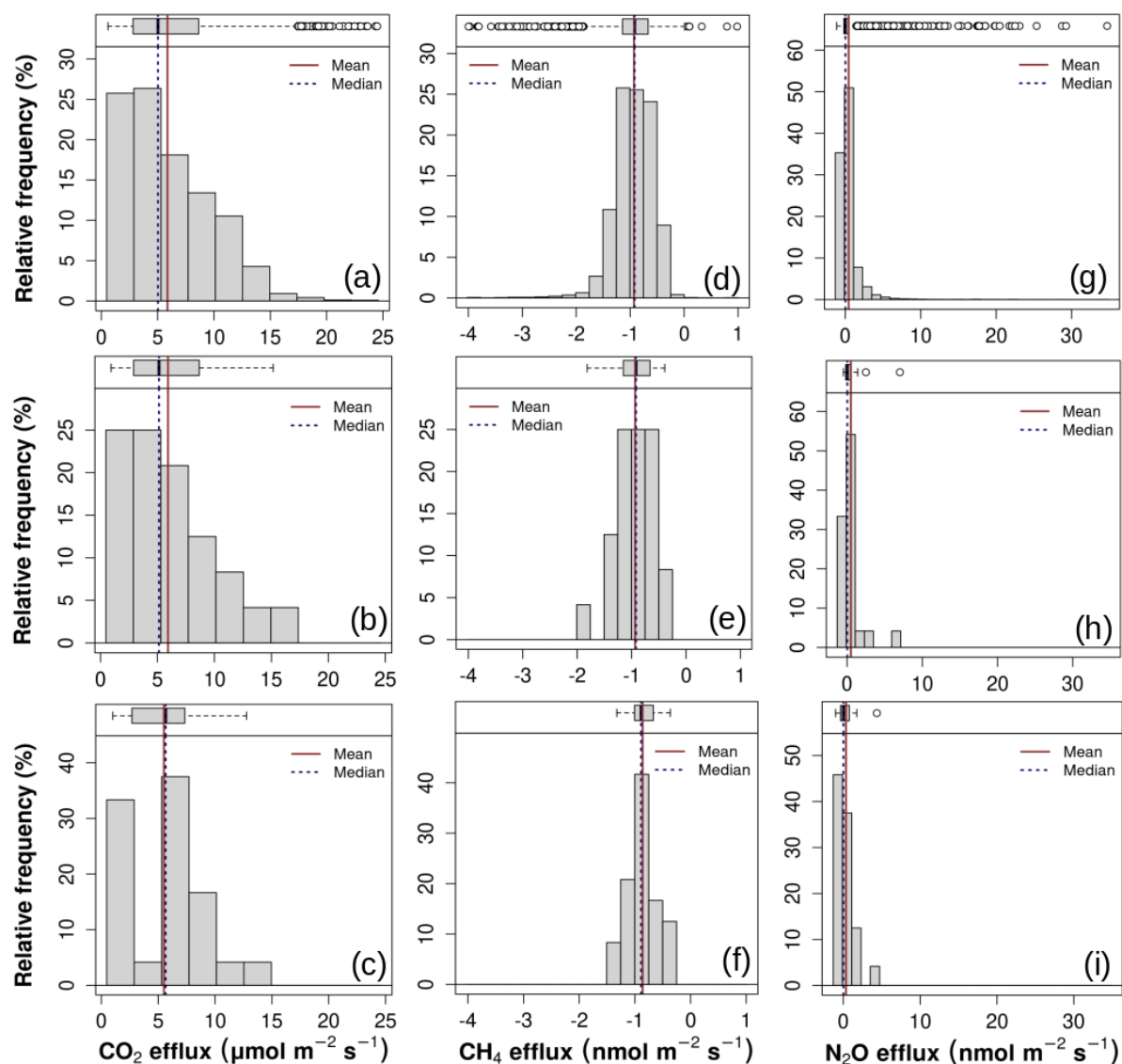
584
585
586
587 **Figure 3**. Histograms for automated measurements of soil CO_2 (F_A CO_2; a), soil CH_4 (F_A
588 CH_4; d̶)̶)̶,̶ and soil N_2O (F_A N_2O; g). Histograms for optimized samples (k=24) using a
589 temporal univariate Latin Hypercube sampling (*tuLHs*) approach for soil CO_2 (b), soil CH_4
590 (e̶)̶)̶,̶ and soil N_2O (h) fluxes. Histograms for fixed temporal stratification (i.e., stratified
591 manual sampling schedule) (k=24) for soil CO_2 (c), soil CH_4 (f̶)̶)̶,̶ and soil N_2O (i) fluxes.
592 ~~Appendix A~~Supplementary material includes results for measurements with k=12 (Fig.
593 ~~A5~~S5) and k=48 (Fig. ~~A6~~S6).
594
595

601
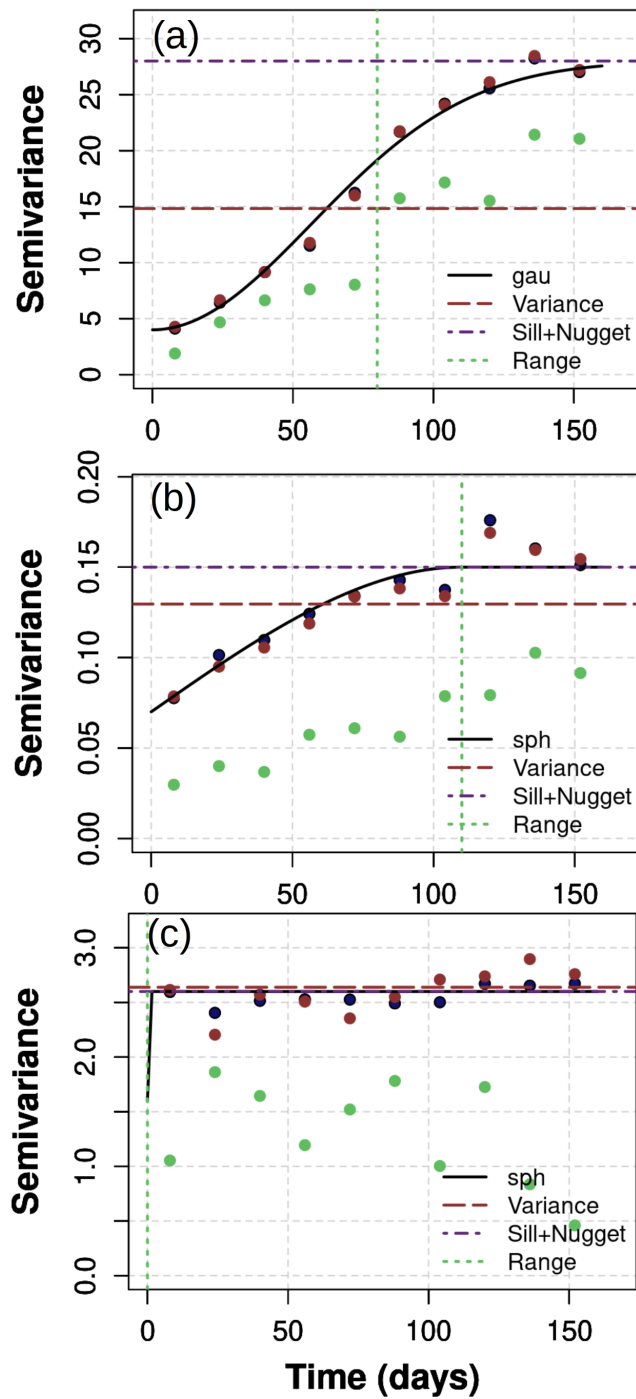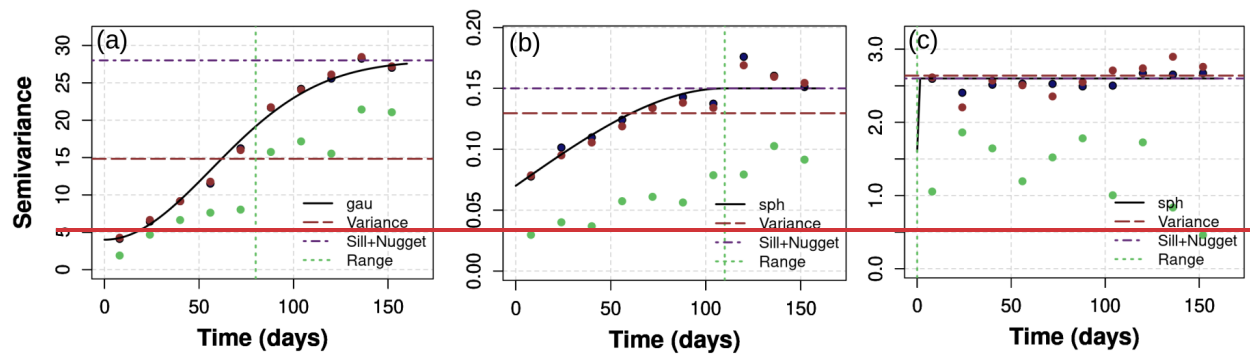
602 **Figure 4**. Comparison of semivariograms between automated measurements (F_A) of soil

603 greenhouse gas fluxes (solid black line) and for optimized samples using a temporal

604 univariate Latin Hypercube sampling (*tuLHs*) approach (red circles) or fixed temporal

605 stratification (green circles) with k=24. Semivarograms are presented for soil CO_2 (a), CH_4

606 (d~~)~~), and N_2O (c) fluxes. Semivariograms for measurements with k=12 and k=48 are

607 ~~presented~~shown in ~~supplementary~~Supplementary Figs. ~~A7~~S7 and ~~A8~~S8, respectively.

608 Semivariogram fits were gaussian (Gau) or spherical (sph).

609

610

611

612
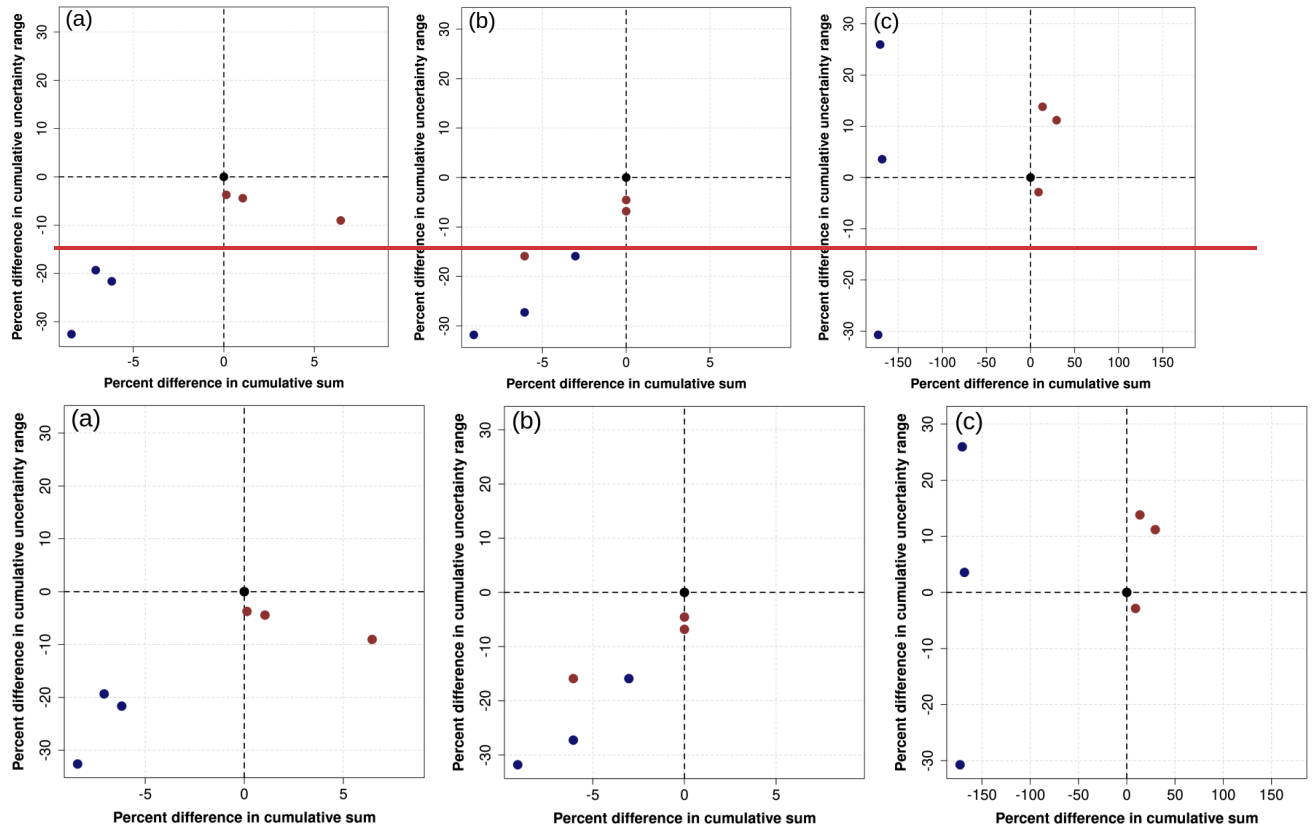
613
614
615
616
617 **Figure 5.** Comparison of percent differences from cumulative sums and associated
618 uncertainty (95% CI) between greenhouse gas fluxes derived from automated measurements
619 (F_A) and using an optimized sampling approach (*tuLHs*) or a fixed temporal stratification.
620 Differences are represented for ~~of~~ soil CO_2 (a), soil CH_4 (b~~)~~), and soil N_2O (c) fluxes.
621 ~~Black~~The black circle in the center (0,0) of a plot represents the values derived from
622 automated measurements (F_A). Blue circles represent estimates from fixed temporal
623 stratification, and red circles represent estimates from an optimized sampling approach
624 (*tuLHs*). Estimates were calculated based on the 258 available automated measurements (Fig.
625 2~~)~~), and numeric estimates are in Table ~~A3~~S3.
626
627
628
629

631

632   **Table A1.** Statistical properties for automated measurements of soil CO_2 (F_ACO_2), soil CH_4
633   (F_ACH_4) and soil N_2O ($F_A N_2O$) fluxes, optimized samples (k=12, 28, 48) using a temporal
634   univariate Latin Hypercube sampling ($tuLHs$), and fixed temporal stratification (k=12, 28,
635   48). Units for soil CO_2 fluxes are in $\mu mol\ m^{-2}\ s^{-1}$, and for soil CH_4 and N_2O fluxes in $nmol\ m^{-2}\ s^{-1}$.

637

	Number of measurements (k)	1st. Quartile	Median	Mean	3rd. Quartile	Standard Deviation
F_ACO_2	8259	2.81	5.03	5.87	8.65	3.85
$tuLHs$ approach (CO_2)	12	3.19	5.30	6.25	8.88	4.06
	24	3.00	5.13	5.93	8.44	3.90
	48	2.84	4.97	5.88	8.54	3.87
Fixed temporal stratification (CO_2)	12	2.68	5.82	5.37	7.10	3.15
	24	2.69	5.66	5.50	7.07	3.24
	48	2.69	5.53	5.45	8.05	3.29
F_ACH_4	8259	-1.14	-0.92	-0.93	-0.67	0.36
$tuLHs$ approach (CH_4)	12	-1.11	-0.89	-0.87	-0.66	0.33
	24	-1.14	-0.92	-0.94	-0.66	0.34
	48	-1.13	-0.91	-0.92	-0.66	0.35
Fixed temporal stratification (CH_4)	12	-1.01	-0.83	-0.83	-0.67	0.27
	24	-1.01	-0.89	-0.86	-0.68	0.26
	48	-1.10	-0.86	-0.88	-0.66	0.29
F_AN_2O	8259	-0.18	0.01	0.45	0.49	1.62
$tuLHs$ approach (N_2O)	12	-0.18	-0.01	0.58	0.50	1.58
	24	-0.18	0.03	0.51	0.45	1.54
	48	-0.17	0.02	0.49	0.45	1.54
Fixed temporal stratification (N_2O)	12	-0.35	0.51	0.59	0.83	1.38
	24	-0.21	-0.08	0.61	0.36	1.97
	48	-0.31	0.00	0.25	0.53	0.91

638

639 **Table A2.** Comparison of errors between experimental variogram for automated
640 measurements of soil greenhouse gases (F_4; k=8259) and experimental variograms for data
641 using temporal univariate Latin Hypercube sampling (*tuLHs*) and fixed temporal
642 stratification.
643

	Approach	Number of measurements (*k*)	Error (Sum of absolute differences)
Soil CO_2 fluxes	Fixed	12	69.31
		24	54.39
		48	49.42
	tuLHs	12	5.69
		24	1.99
		48	1.39
Soil CH_4 fluxes	Fixed	12	0.63
		24	0.68
		48	0.49
	tuLHs	12	0.06
		24	0.04
		48	0.02
Soil N_2O fluxes	Fixed	12	10.01
		24	12.25
		48	16.75
	tuLHs	12	0.82
		24	1.13
		48	3.57

644

645
646
647

648 **Table A3.** Cumulative sum and associated uncertainty of greenhouse gas (GHG) fluxes
649 derived from automated measurements (F_A) and using an optimized sampling approach
650 (*tuLHs*) or a fixed temporal stratification. Cumulative sum represents the total flux from
651 available measurements derived from automated measurements for all GHG fluxes.

	Number of measurements (*k*)	Cumulative Sum	Uncertainty 95% CI		Uncertainty Range
$F_A CO_2$ (g CO_2 m^2)	8259	5758	893	13860	12966
tuLHs approach (g CO_2 m^2)	12	6130	1423	13218	11794
	24	5818	1046	13438	12391
	48	5766	946	13429	12482
Fixed temporal stratification (g CO_2 m^2)	12	5273	1376	10117	8740
	24	5402	1196	11356	10160
	48	5351	1162	11621	10458
$F_A CH_4$ (g CH_4 m^2)	8259	-0.33	-0.58	-0.14	0.44
tuLHs approach (g CH_4 m^2)	12	-0.31	-0.49	-0.12	0.37
	24	-0.33	-0.57	-0.16	0.41
	48	-0.33	-0.56	-0.14	0.42
Fixed temporal stratification (g CH_4 m^2)	12	-0.3	-0.45	-0.15	0.3
	24	-0.31	-0.46	-0.14	0.32
	48	-0.32	-0.51	-0.14	0.37
$F_A N_2O$ (g N_2O m^2)	8259	0.44	-0.53	3.67	4.2
tuLHs approach (g N_2O m^2)	12	0.57	-0.48	4.19	4.67
	24	0.5	-0.43	4.35	4.78
	48	0.48	-0.5	3.58	4.08
	12	-0.3	-0.83	3.52	4.35
	24	-0.31	-0.43	4.86	5.29

Fixed temporal stratification (g N_2O m^2)	48		-0.7	2.21
		-0.32		2.91

654
655

656

657
658
659
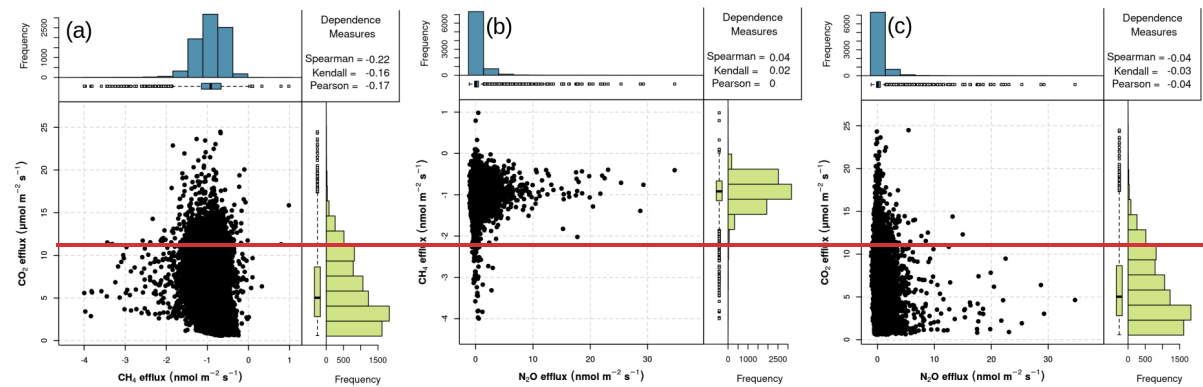
660
661
662 **Figure A1.** Relationships between soil CO_2 ($F_A CO_2$) with soil CH_4 ($F_A CH_4$) fluxes (a), soil
663 CH_4 ($F_A CH_4$) with soil N_2O ($F_A N_2O$) fluxes (b), and soil CO_2 ($F_A CO_2$) with soil N_2O (F_A
664 N_2O) fluxes. None of these relationships were significant at $\alpha = 0.05$. These relationships were
665 derived using all available data from automated measurements (F_A) of soil greenhouse gas
666 fluxes.
667

668
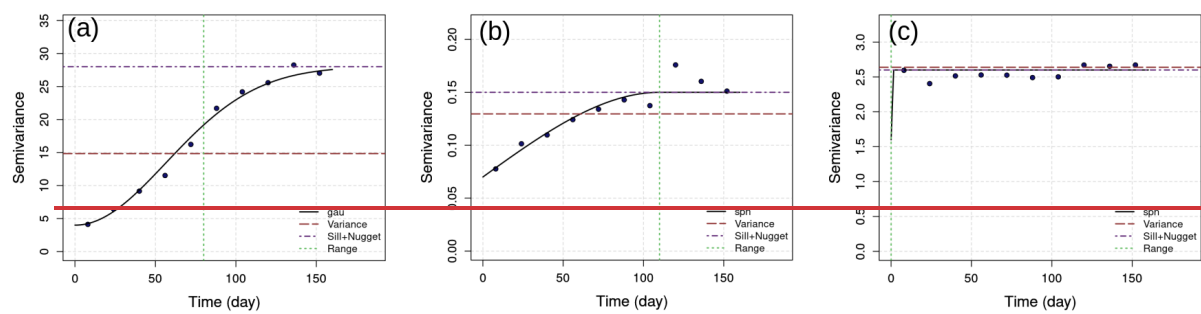
669
670
671 **Figure A2.** Semivariograms of soil CO_2 ($F_A CO_2$; a), soil CH_4 ($F_A CH_4$; b) and soil N_2O (F_A
672 N_2O; c) fluxes. These semivariograms were derived using all available data from automated
673 measurements (F_A) of soil greenhouse gas fluxes. Semivariogram fits were gaussian (Gau) or
674 spherical (sph).
675
676

677
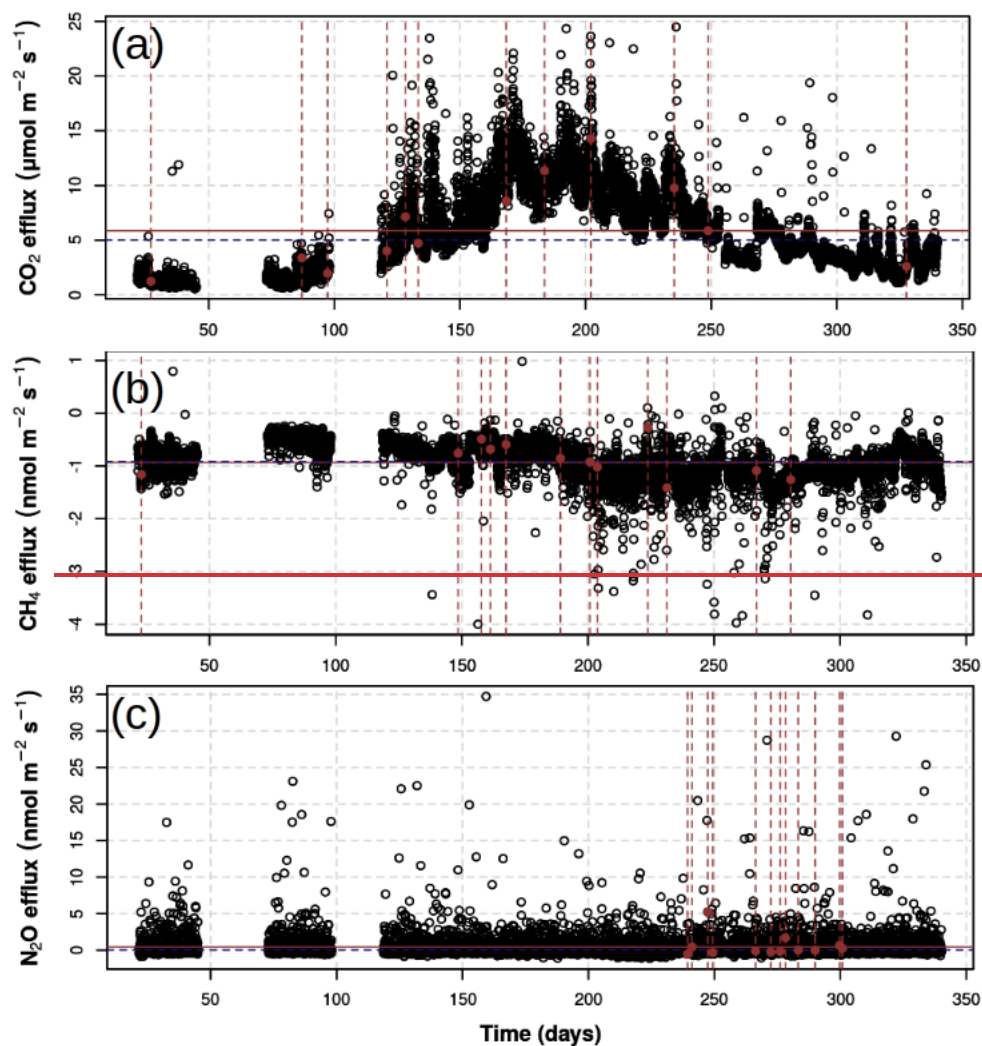
678
679
680 **Figure A3.** Time series of automated measurements (FA) of soil greenhouse gas fluxes
681 (black circles) and optimized samples (k=12) using a temporal univariate Latin Hypercube
682 sampling (*tuLHs*) approach for soil CO_2 (a), soil CH_4 (b) and soil N_2O (c) fluxes. Horizontal
683 red line represents the mean and horizontal blue line the median of each greenhouse gas flux
684 derived from automated measurements.
685
686
687
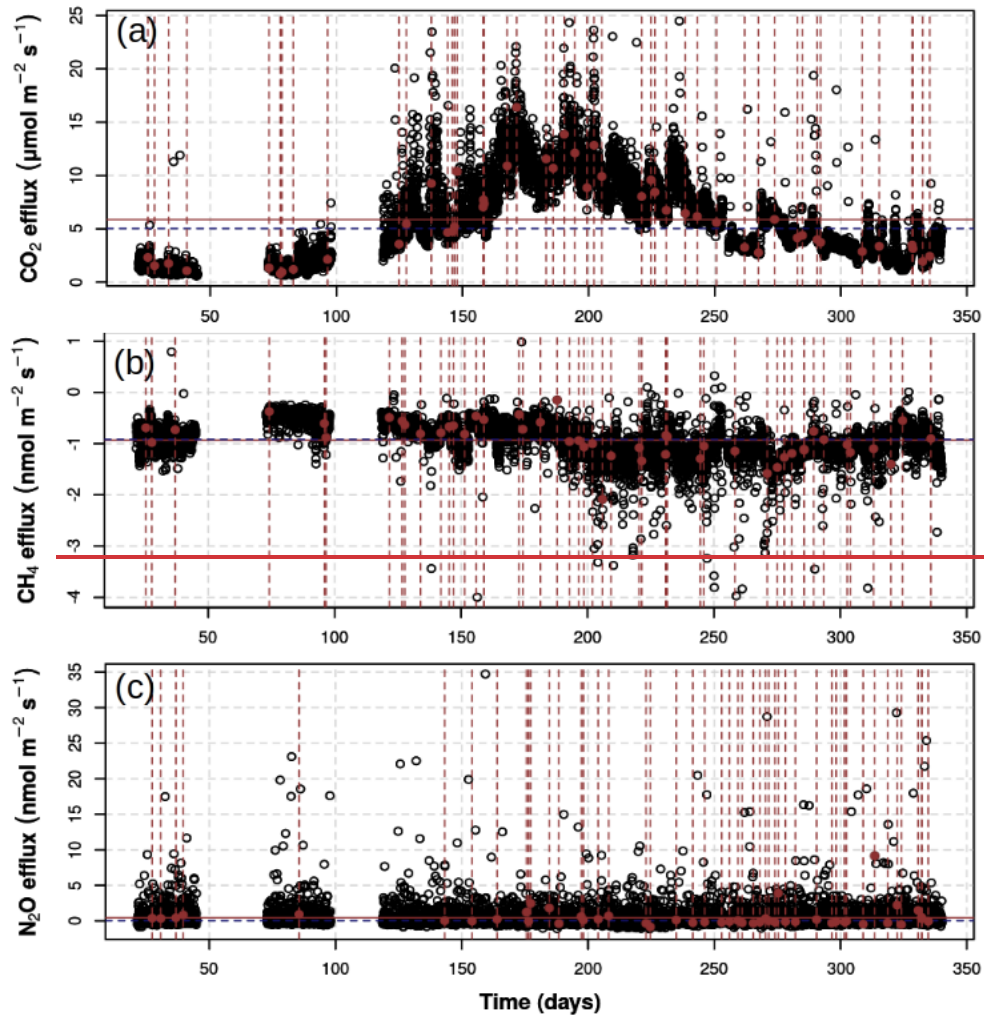
Figure A4. Time series of automated measurements (FA) of soil greenhouse gas fluxes (black circles) and optimized samples (*k*=48) using a temporal univariate Latin Hypercube sampling (*tuLHs*) approach for soil CO_2 (a), soil CH_4 (b) and soil N_2O (c) fluxes. Horizontal red line represents the mean and horizontal blue line the median of each greenhouse gas flux derived from automated measurements.
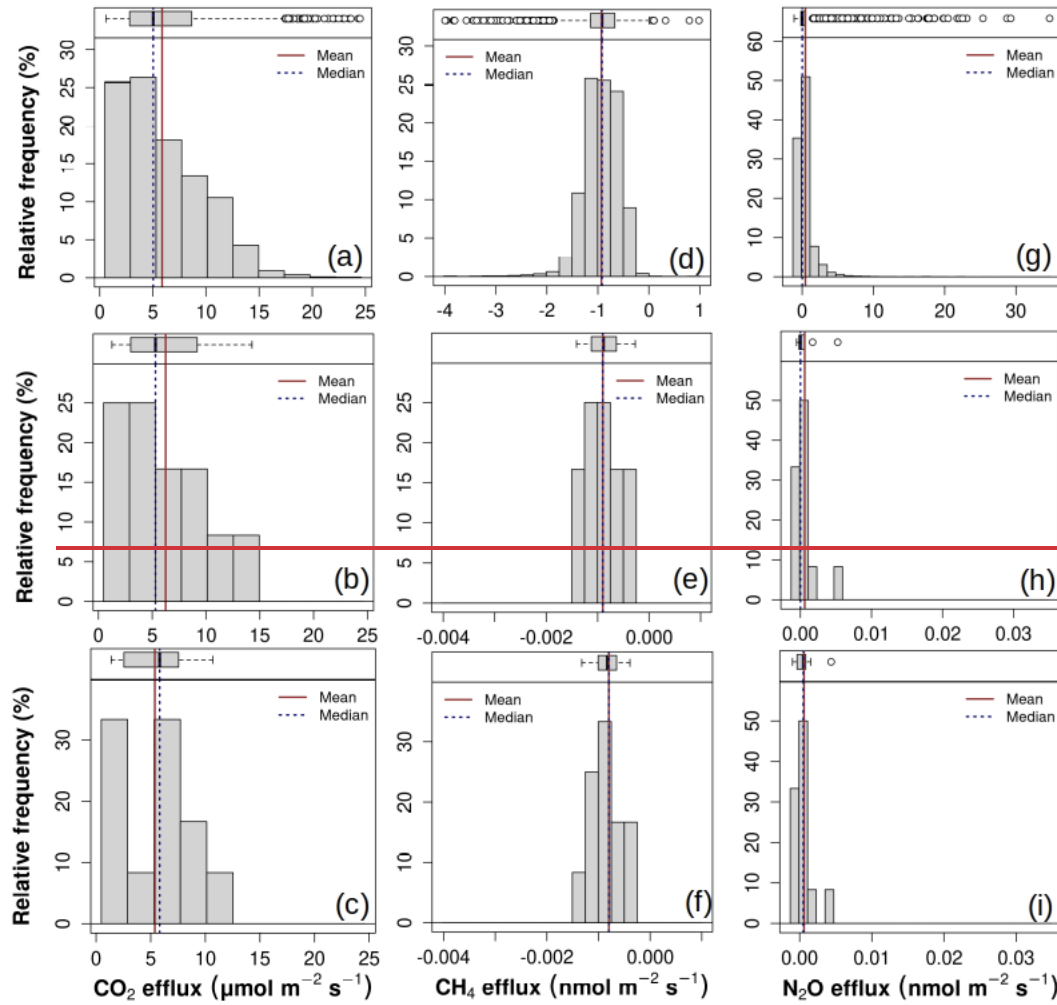
709
710
711 **Figure A5.** Histograms for automated measurements of soil CO_2 (F_A CO_2; a), soil CH_4 (F_A
712 CH_4; d) and soil N_2O (F_A N_2O; g) fluxes. Histograms for optimized samples ($k=12$) using a
713 temporal univariate Latin Hypercube sampling (*tuLHs*) approach for soil CO_2 (b), soil CH_4
714 (e) and soil N_2O (h) fluxes. Histograms for fixed temporal stratification (i.e., stratified
715 manual sampling schedule; $k=12$) for soil CO_2 (c), soil CH_4 (f) and soil N_2O (i) fluxes.
716
717
718
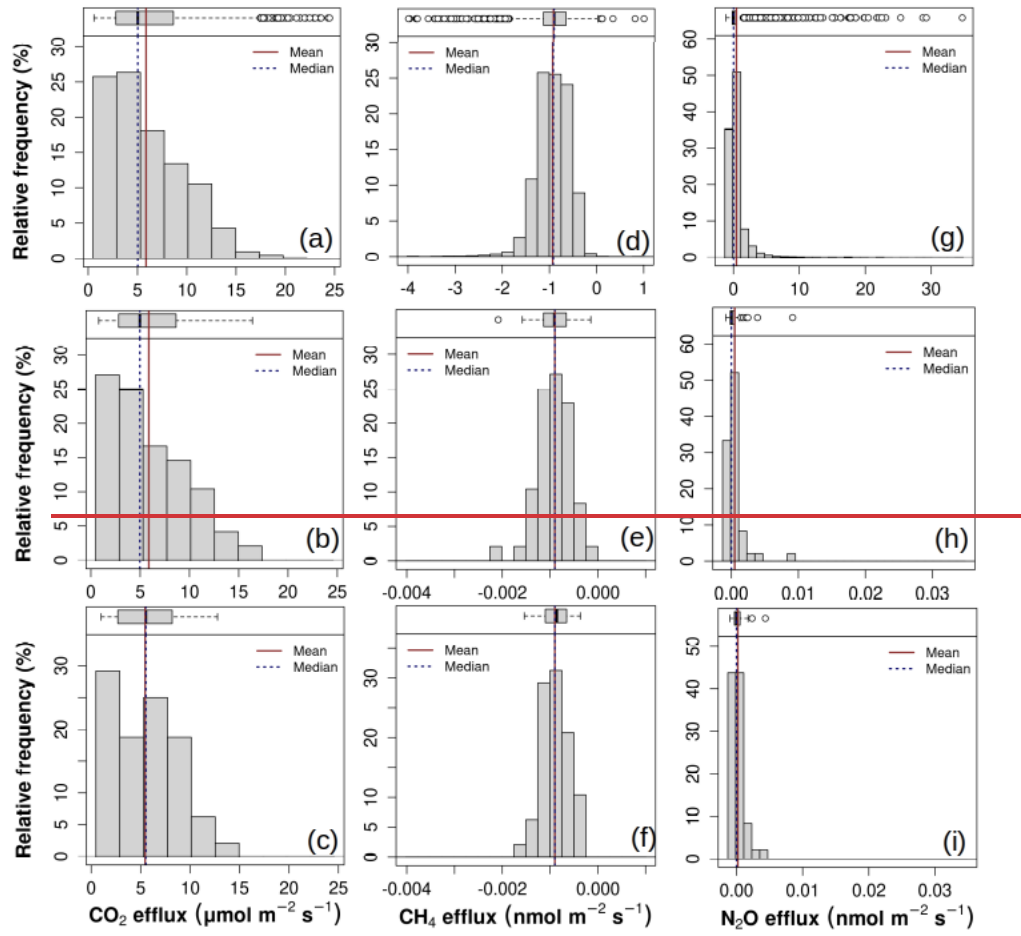
Figure A6. Histograms for automated measurements of soil CO_2 (F_A CO_2; a), soil CH_4 (F_A CH_4; d) and soil N_2O (F_A N_2O; g) fluxes. Histograms for optimized samples (k=48) using a temporal univariate Latin Hypercube sampling (*tuLHs*) approach for soil CO_2 (b), soil CH_4 (e) and soil N_2O (h) fluxes. Histograms for fixed temporal stratification (i.e., stratified manual sampling schedule; k=48) for soil CO_2 (c), soil CH_4 (f) and soil N_2O (i) fluxes.

729
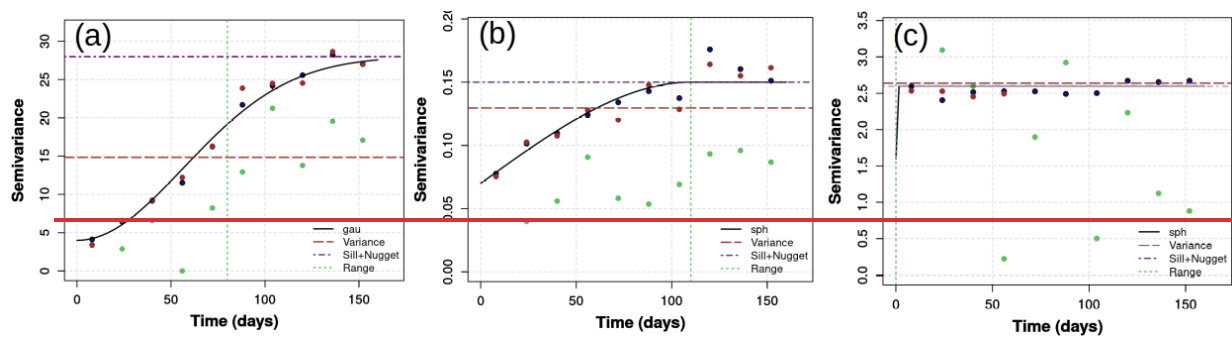
730
731
732 **Figure A7.** Comparison of semivariograms between automated measurements (F_A) of soil
733 greenhouse gas fluxes (solid black line) and for optimized (red circles) or fixed temporal
734 stratification (green circles) with k=12. Semivarograms are presented for soil CO_2 (a), CH_4
735 (d) and N_2O (c) fluxes. Semivariogram fits were gaussian (Gau) or spherical (sph).
736
737
738
739
740
741

742
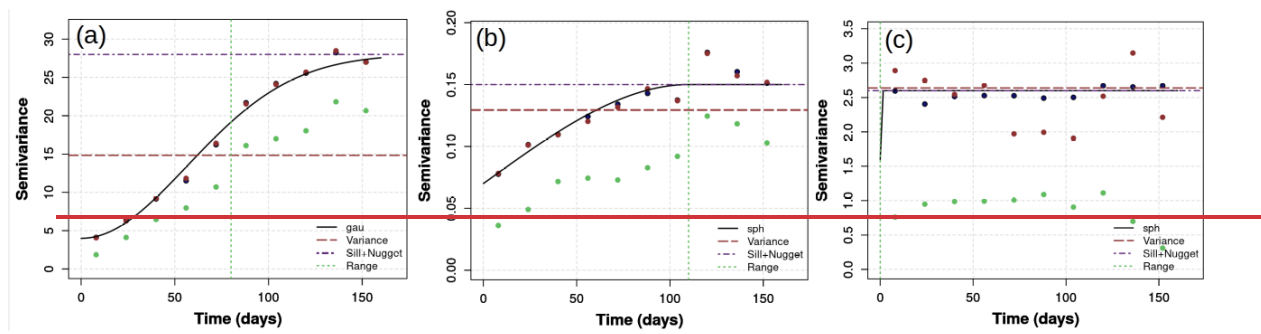
743
744
745 **Figure A8.** Comparison of semivariograms between automated measurements (F_A) of soil
746 greenhouse gas fluxes (solid black line) and for optimized (red circles) or fixed temporal
747 stratification (green circles) with $k=48$. Semivarograms are presented for soil CO_2 (a), CH_4
748 (d) and N_2O (c) fluxes. Semivariogram fits were gaussian (Gau) or spherical (sph).
749
750
751

References

752

~~Anderegg, W. R. L.: Gambling With the Climate: How Risky of a Bet Are Natural Climate~~ 753

~~Solutions?, https://doi.org/10.1029/2021AV000490, September 2021.~~ 754

Bahn, M., Reichstein, M., Davidson, E. A., Gruenzweig, J., Jung, M., Carbone, M. S., Epron, 755

D., Misson, L., Nouvellon, Y., Roupsard, O., Savage, K., Trumbore, S. E., Gimeno, C., 756

Curiel Yuste, J., Tang, J., Vargas, R., and Janssens, I. A.: Soil respiration at mean annual 757

temperature predicts annual total across vegetation types and biomes, Biogeosciences, 7, 758

2147–2157, 2010. 759

Ball, B. C.: Soil structure and greenhouse gas emissions: a synthesis of 20 years of 760

experimentation, Eur. J. Soil Sci., 64, 357–373, 2013. 761

Barba, J., Poyatos, R., and Vargas, R.: Automated measurements of greenhouse gases fluxes 762

from tree stems and soils: magnitudes, patterns and drivers, Sci. Rep., 9, 4005, 2019. 763

Barba, J., Poyatos, R., Capooci, M., and Vargas, R.: Spatiotemporal variability and origin of 764

CO2 and CH4 tree stem fluxes in an upland forest, Glob. Chang. Biol., 27, 4879–4893, 2021. 765

Bond-Lamberty, B., Christianson, D. S., Malhotra, A., Pennington, S. C., Sihi, D., 766

AghaKouchak, A., Anjileli, H., Altaf Arain, M., Armesto, J. J., Ashraf, S., Ataka, M., 767

Baldocchi, D., Andrew Black, T., Buchmann, N., Carbone, M. S., Chang, S., Crill, P., Curtis, 768

P. S., Davidson, E. A., Desai, A. R., Drake, J. E., El-Madany, T. S., Gavazzi, M., Görres, C., 769

Gough, C. M., Goulden, M., Gregg, J., Gutiérrez del Arroyo, O., He, J., Hirano, T., Hopple, 770

A., Hughes, H., Järveoja, J., Jassal, R., Jian, J., Kan, H., Kaye, J., Kominami, Y., Liang, N., 771

Lipson, D., Macdonald, C. A., Maseyk, K., Mathes, K., Mauritz, M., Mayes, M. A., 772

McNulty, S., Miao, G., Migliavacca, M., Miller, S., Miniat, C. F., Nietz, J. G., Nilsson, M. 773

B., Noormets, A., Norouzi, H., O'Connell, C. S., Osborne, B., Oyonarte, C., Pang, Z., Peichl, 774

775 M., Pendall, E., Perez-Quezada, J. F., Phillips, C. L., Phillips, R. P., Raich, J. W., Renchon,

776 A. A., Ruehr, N. K., Sánchez-Cañete, E. P., Saunders, M., Savage, K. E., Schrumpf, M.,

777 Scott, R. L., Seibt, U., Silver, W. L., Sun, W., Szutu, D., Takagi, K., Takagi, M., Teramoto,

778 M., Tjoelker, M. G., Trumbore, S., Ueyama, M., Vargas, R., Varner, R. K., Verfaillie, J.,

779 Vogel, C., Wang, J., Winston, G., Wood, T. E., Wu, J., Wutzler, T., Zeng, J., Zha, T., Zhang,

780 Q., and Zou, J.: COSORE: A community database for continuous soil respiration and other

781 soil-atmosphere greenhouse gas flux data, Glob. Chang. Biol., 249, 434, 2020.

782 Bossio, D. A., Cook-Patton, S. C., Ellis, P. W., Fargione, J., Sanderman, J., Smith, P., Wood,

783 S., Zomer, R. J., von Unger, M., Emmer, I. M., and Griscom, B. W.: The role of soil carbon

784 in natural climate solutions, Nature Sustainability, 3, 391–398, 2020.

785 Bouma, J.: Chapter 4 - Implications of the Knowledge Paradox for Soil Science, in:

786 Advances in Agronomy, vol. 106, edited by: Sparks, D. L., Academic Press, 143–171, 2010.

787 Bowden, R. D., Castro, M. S., Melillo, J. M., Steudler, P. A., and Aber, J. D.: Fluxes of

788 greenhouse gases between soils and the atmosphere in a temperate forest following a

789 simulated hurricane blowdown, Biogeochemistry, 21, 61–71, 1993.

790 Bowden, R. D., Newkirk, K. M., and Rullo, G. M.: Carbon dioxide and methane fluxes by a

791 forest soil under laboratory-controlled moisture and temperature conditions, Soil Biol.

792 Biochem., 30, 1591–1597, 1998.

793 Bréchet, L. M., Daniel, W., Stahl, C., Burban, B., Goret, J.-Y., Salomón, R. L., and Janssens,

794 I. A.: Simultaneous tree stem and soil greenhouse gas (CO_2 , CH_4 , N_2O) flux

795 measurements: a novel design for continuous monitoring towards improving flux estimates

796 and temporal resolution, New Phytol., 230, 2487–2500, 2021.

797   Butterbach-Bahl, K., Kock, M., Willibald, G., Hewett, B., Buhagiar, S., Papen, H., and Kiese,

798   R.: Temporal variations of fluxes of NO, NO2, N2O, CO2, and CH4in a tropical rain forest

799   ecosystem, Global Biogeochem. Cycles, 18, https://doi.org/10.1029/2004gb002243, 2004.

800   Capooci, M. and Vargas, R.: Diel and seasonal patterns of soil CO2 efflux in a temperate

801   tidal marsh, Sci. Total Environ., 802, 149715, ~~2022~~2022a.

802   Capooci, M. and Vargas, R.: Trace gas fluxes from tidal salt marsh soils: implications for

803   carbon--sulfur biogeochemistry, Biogeosciences, 19, 4655–4670, 2022b.

804   Capooci, M., Barba, J., Seyfferth, A. L., and Vargas, R.: Experimental influence of storm-

805   surge salinity on soil greenhouse gas emissions from a tidal salt marsh, Sci. Total Environ.,

806   686, 1164–1172, 2019.

807   Castro, M. S., Melillo, J. M., Steudler, P. A., and Chapman, J. W.: Soil moisture as a

808   predictor of methane uptake by temperate forest soils, Can. J. For. Res., 24, 1805–1810,

809   1994.

810   Castro, M. S., Steudler, P. A., Melillo, J. M., Aber, J. D., and Bowden, R. D.: Factors

811   controlling atmospheric methane consumption by temperate forest soils, Global Biogeochem.

812   Cycles, 9, 1–10, 1995.

813   Chilès, J.-P. and Delfiner, P.: Geostatistics: Modeling Spatial Uncertainty, John Wiley &

814   Sons, 720 pp., 2009.

815   Cueva, A., Bullock, S. H., López-Reyes, E., and Vargas, R.: Potential bias of daily soil CO2

816   efflux estimates due to sampling time, Sci. Rep., 7, 11925, 2017.

Freeman, C., Lock, M. A., and Reynolds, B.: Fluxes of CO2, CH4 and N2O from a Welsh peatland following simulation of water table draw-down: Potential feedback to climatic change, Biogeochemistry, 19, https://doi.org/10.1007/bf00000574, 1993.

Griscom, B. W., Adams, J., Ellis, P. W., Houghton, R. A., Lomax, G., Miteva, D. A., Schlesinger, W. H., Shoch, D., Siikamäki, J. V., Smith, P., Woodbury, P., Zganjar, C., Blackman, A., Campari, J., Conant, R. T., Delgado, C., Elias, P., Gopalakrishna, T., Hamsik, M. R., Herrero, M., Kiesecker, J., Landis, E., Laestadius, L., Leavitt, S. M., Minnemeyer, S., Polasky, S., Potapov, P., Putz, F. E., Sanderman, J., Silvius, M., Wollenberg, E., and Fargione, J.: Natural climate solutions, Proc. Natl. Acad. Sci. U. S. A., 114, 11645–11650, 2017.

Gunawardana, A., Meek, C., and Xu, P.: A model for temporal dependencies in event streams, Adv. Neural Inf. Process. Syst., 24, 2011.

Hao, W. M., Scharffe, D., Crutzen, P. J., and Sanhueza, E.: Production of N2O, CH4, and CO2 from soils in the tropical savanna during the dry season, J. Atmos. Chem., 7, 93–105, 1988.

Hill, A. C., Barba, J., Hom, J., and Vargas, R.: Patterns and drivers of multi-annual CO2 emissions within a temperate suburban neighborhood, Biogeochemistry, 152, 35–50, 2021.

Huntington, D. E. and Lyrintzis, C. S.: Improvements to and limitations of Latin hypercube sampling, Probab. Eng. Mech., 13, 245–253, 1998.

Hutchinson, G. E.: The Concept of Pattern in Ecology, Proceedings of the Academy of Natural Sciences of Philadelphia, 105, 1–12, 1953.

838 Jian, J., Vargas, R., Anderson-Teixeira, K., Stell, E., Herrmann, V., Horn, M., Kholod, N.,

839 Manzon, J., Marchesi, R., Paredes, D., and Bond-Lamberty, B.: A restructured and updated

840 global soil respiration database (SRDB-V5), Data, Algorithms, and Models,

841 https://doi.org/10.5194/essd-2020-136, 2020.

842 Keller, M., Kaplan, W. A., and Wofsy, S. C.: Emissions of N2O, CH4 and CO2 from tropical

843 forest soils, J. Geophys. Res., 91, 11791, 1986.

844 Kim, D. G., Vargas, R., Bond-Lamberty, B., and Turetsky, M. R.: Effects of soil rewetting

845 and thawing on soil gas fluxes: a review of current literature and suggestions for future

846 research, Biogeosciences, 9, 2459–2483, 2012.

847 Le, V. H., Díaz-Viera, M. A., Vázquez-Ramírez, D., del Valle-García, R., Erdely, A., and

848 Grana, D.: Bernstein copula-based spatial cosimulation for petrophysical property prediction

849 conditioned to elastic attributes, J. Pet. Sci. Eng., 193, 107382, 2020.

850 Lucas-Moffat, A. M., Huth, V., Augustin, J., Brümmer, C., Herbst, M., and Kutsch, W. L.:

851 Towards pairing plot and field scale measurements in managed ecosystems: Using eddy

852 covariance to cross-validate CO2 fluxes modeled from manual chamber campaigns, Agric.

853 For. Meteorol., 256–257, 362–378, 2018.

854 Luo, G. J., Kiese, R., Wolf, B., and Butterbach-Bahl, K.: Effects of soil temperature and

855 moisture on methane uptake and nitrous oxide emissions across three different ecosystem

856 types, Biogeosciences, 10, 3205–3219, 2013.

857 Murguia-Flores, F., Arndt, S., Ganesan, A. L., Murray-Tortarolo, G., and Hornibrook, E. R.

858 C.: Soil Methanotrophy Model (MeMo v1.0): a process-based model to quantify global

859 uptake of atmospheric methane by soil, Geosci. Model Dev., 11, 2009–2032, 2018.

860 Oertel, C., Matschullat, J., Zurba, K., Zimmermann, F., and Erasmi, S.: Greenhouse gas

861 emissions from soils—A review, Geochem. Explor. Environ. Analy., 76, 327–352, 2016.

862 Ojanen, P., Minkkinen, K., Alm, J., and Penttilä, T.: Soil–atmosphere CO_2, CH_4 and N_2O

863 fluxes in boreal forestry-drained peatlands, For. Ecol. Manage., 260, 411–421, 2010.

864 Petrakis, S., Seyfferth, A., Kan, J., Inamdar, S., and Vargas, R.: Influence of experimental

865 extreme water pulses on greenhouse gas emissions from soils, Biogeochemistry, 133, 147–

866 164, 2017.

867 Petrakis, S., Barba, J., Bond-Lamberty, B., and Vargas, R.: Using greenhouse gas fluxes to

868 define soil functional types, Plant Soil, 423, 285–294, 2018.

869 Phillips, C. L., Bond-Lamberty, B., Desai, A. R., Lavoie, M., Risk, D., Tang, J. W., Todd-

870 Brown, K., and Vargas, R.: The value of soil respiration measurements for interpreting and

871 modeling terrestrial carbon cycling, Plant Soil, 413, 1–25, 2017.

872 Pyrcz, M. J. and Deutsch, C. V.: Geostatistical Reservoir Modeling, OUP USA, 433 pp.,

873 2014.

874 Rowlings, D. W., Grace, P. R., Kiese, R., and Weier, K. L.: Environmental factors

875 controlling temporal and spatial variability in the soil-atmosphere exchange of CO_2, CH_4

876 and N_2O from an Australian subtropical rainforest, Glob. Chang. Biol., 18, 726–738, 2012.

877 Savage, K., Phillips, R., and Davidson, E.: High temporal frequency measurements of

878 greenhouse gas emissions from soils, Biogeosciences, 11, 2709–2720, 2014.

879 Shakoor, A., Shahbaz, M., Farooq, T. H., Sahar, N. E., Shahzad, S. M., Altaf, M. M., and

880 Ashraf, M.: A global meta-analysis of greenhouse gases emission and crop yield under no-

881 tillage as compared to conventional tillage, Sci. Total Environ., 750, 142299, 2021.

882   Storn, R. and Price, K.: Differential Evolution – A Simple and Efficient Heuristic for global

883   Optimization over Continuous Spaces, J. Global Optimiz., 11, 341–359, 1997.

884   Tallec, T., Brut, A., Joly, L., Dumelié, N., Serça, D., Mordelet, P., Claverie, N., Legain, D.,

885   Barrié, J., Decarpenterie, T., Cousin, J., Zawilski, B., Ceschia, E., Guérin, F., and Le Dantec,

886   V.: N2O flux measurements over an irrigated maize crop: A comparison of three methods,

887   Agric. For. Meteorol., 264, 56–72, 2019.

888   Tang, X., Liu, S., Zhou, G., Zhang, D., and Zhou, C.: Soil-atmospheric exchange of CO2 ,

889   CH4 , and N2 O in three subtropical forest ecosystems in southern China, Glob. Chang. Biol.,

890   12, 546–560, 2006.

891   Team, RC and Others: R: A language and environment for statistical computing, 2013.

892   Trangmar, B. B., Yost, R. S., and Uehara, G.: Application of Geostatistics to Spatial Studies

893   of Soil Properties, in: Advances in Agronomy, vol. 38, edited by: Brady, N. C., Academic

894   Press, 45–94, 1986.

895   Ullah, S. and Moore, T. R.: Biogeochemical controls on methane, nitrous oxide, and carbon

896   dioxide fluxes from deciduous forest soils in eastern Canada, J. Geophys. Res., 116,

897   https://doi.org/10.1029/2010jg001525, 2011.

898   Vargas, R.: How a hurricane disturbance influences extreme CO2 fluxes and variance in a

899   tropical forest, Environ. Res. Lett., 2012.

900   Vargas, R., Carbone, M. S., Reichstein, M., and Baldocchi, D. D.: Frontiers and challenges in

901   soil respiration research: from measurements to model-data integration, Biogeochemistry,

902   102, 1–13, 2011.

903   Vargas, R., Sánchez-Cañete P., E., Serrano-Ortiz, P., Curiel Yuste, J., Domingo, F., López-

904   Ballesteros, A., and Oyonarte, C.: Hot-Moments of Soil CO2 Efflux in a Water-Limited

905   Grassland, Soil Systems, 2, 47, 2018.

906   Vicca, S., Bahn, M., Estiarte, M., van Loon, E. E., Vargas, R., Alberti, G., Ambus, P., Arain,

907   M. A., Beier, C., Bentley, L. P., Borken, W., Buchmann, N., Collins, S. L., de Dato, G.,

908   Dukes, J. S., Escolar, C., Fay, P., Guidolotti, G., Hanson, P. J., Kahmen, A., Kröel-Dulay, G.,

909   Ladreiter-Knauss, T., Larsen, K. S., Lellei-Kovacs, E., Lebrija-Trejos, E., Maestre, F. T.,

910   Marhan, S., Marshall, M., Meir, P., Miao, Y., Muhr, J., Niklaus, P. A., Ogaya, R., Peñuelas,

911   J., Poll, C., Rustad, L. E., Savage, K., Schindlbacher, A., Schmidt, I. K., Smith, A. R., Sotta,

912   E. D., Suseela, V., Tietema, A., van Gestel, N., van Straaten, O., Wan, S., Weber, U., and

913   Janssens, I. A.: Can current moisture responses predict soil CO2 efflux under altered

914   precipitation regimes? A synthesis of manipulation experiments, Biogeosciences, 11, 2991–

915   3013, 2014.

916   Villarreal, S., Guevara, M., Alcaraz-Segura, D., and Vargas, R.: Optimizing an

917   Environmental Observatory Network Design Using Publicly Available Data, J. Geophys.

918   Res. Biogeosci., 124, 1812–1826, 2019.

919   Wang, G. and Chen, S.: A review on parameterization and uncertainty in modeling

920   greenhouse gas emissions from soil, Geoderma, 170, 206–216, 2012.

921   Warner, D. L., Guevara, M., Inamdar, S., and Vargas, R.: Upscaling soil-atmosphere CO2

922   and CH4 fluxes across a topographically complex forested landscape, Agricultural and forest,

923   264, 80–91, 2019.

924   Werner, C., Kiese, R., and Butterbach-Bahl, K.: Soil-atmosphere exchange of N2O, CH4,

925   and CO2and controlling environmental factors for tropical rain forest sites in western Kenya,

926   J. Geophys. Res., 112, https://doi.org/10.1029/2006jd007388, 2007.

927   Wu, X., Brüggemann, N., Gasche, R., Shen, Z., Wolf, B., and Butterbach-Bahl, K.:

928   Environmental controls over soil-atmosphere exchange of N2O, NO, and CO2in a temperate

929   Norway spruce forest, Global Biogeochem. Cycles, 24,

930   https://doi.org/10.1029/2009gb003616, 2010.

931   Yao, Z., Zheng, X., Xie, B., Liu, C., Mei, B., Dong, H., Butterbach-Bahl, K., and Zhu, J.:

932   Comparison of manual and automated chambers for field measurements of N2O, CH4, CO2

933   fluxes from cultivated land, Atmos. Environ., 43, 1888–1896, 2009.